PAPERS IN PHYSICAL OCEANOGRAPHY AND METEOROLOGY

PUBLISHED BY

MASSACHUSETTS INSTITUTE OF TECHNOLOGY

AND

WOODS HOLE OCEANOGRAPHIC INSTITUTION

VOL. XI, No. 4

THE ANALYSIS OF TIDAL PHENOMENA IN NARROW EMBAYMENTS

BY

ALFRED C. REDFIELD

CAMBRIDGE AND WOODS HOLE, MASSACHUSETTS

JULY, 1950

PAPERS IN PHYSICAL OCEANOGRAPHY AND METEOROLOGY

(In continuation of Meteorological Papers)

Meteorological Papers

Vol. I,	No. 1.	H. C. Willett: Synoptic Studies in Fog, 1930.	Out of Print
	No. 2.	Horace R. Byers: Characteristic Weather Phenomena of California, 1931.	1.00*
	No. 3.	C.-G. Rossby: Thermodynamics Applied to Air Mass Analysis, 1932.	1.00*
	No. 4.	C.-G. Rossby: A Generalization of the Theory of the Mixing Length with Applications to Atmospheric and Oceanic Turbulence, 1932.	Out of Print

Papers in Physical Oceanography and Meteorology

Vol. II,	No. 1.	H. U. Sverdrup and F. M. Soule: Scientific Results of the "Nautilus" Expedition, 1931, Parts I to III, 1933.	1.00†
	No. 2.	H. C. Willett: American Air Mass Properties, 1933.	1.00*
	No. 3.	B. Villinger and Henry C. Stetson: Scientific Results of the "Nautilus" Expedition, 1931, Parts IV and V, 1933.	Out of Print
	No. 4.	Henry B. Bigelow: Studies of the Waters on the Continental Shelf, Cape Cod to Chesapeake Bay, I. The Cycle of Temperature, 1933.	1.00†
Vol. III,	No. 1.	H. R. Seiwell: The Distribution of Oxygen in the Western Basin of the North Atlantic, 1934.	1.00†
	No. 2.	K. O. Lange and C. S. Draper: The Meteorological Airplane Ascents of the Massachusetts Institute of Technology, 1934.	Out of Print
	No. 3.	C.-G. Rossby and R. B. Montgomery: The Layer of Frictional Influence in Wind and Ocean Currents, 1935.	Out of Print
	No. 4.	H. R. Seiwell: The Cycle of Phosphorus in the Western Basin of the North Atlantic, I. Phosphate Phosphorus, 1935.	1.00†
Vol. IV,	No. 1.	Henry B. Bigelow and Mary Sears: Studies of the Waters on the Continental Shelf, Cape Cod to Chesapeake Bay, II. Salinity, 1935.	1.00†
	No. 2.	H. C. Willett: Discussion and Illustration of Problems Suggested by the Analysis of Atmospheric Cross-Sections, 1935.	Out of Print
	No. 3.	C.-G. Rossby and R. B. Montgomery: On the Momentum Transfer at the Sea Surface, 1936.	Out of Print
	No. 4.	C. O'D. Iselin: A Study of the Circulation of the Western North Atlantic, 1936.	1.00†
Vol. V,	No. 1.	C.-G. Rossby: Dynamics of Steady Ocean Currents in the Light of Experimental Fluid Mechanics, 1936.	1.00*
	No. 2.	H. R. Seiwell: Short Period Vertical Oscillations in the Western Basin of the North Atlantic, 1937.	0.75†
	No. 3.	H. R. Seiwell: The Minimum Oxygen Concentration in the Western Basin of the North Atlantic, 1937.	0.50†
	No. 4.	Henry C. Stetson: The Sediments of the Continental Shelf off the Eastern Coast of the United States, 1938.	Out of Print

(*Continued on inside back cover*)

* Requests for this number should be addressed to Meteorological Department, Massachusetts Institute of Technology, Cambridge, Massachusetts.

† Requests for this number should be addressed to Woods Hole Oceanographic Institution, Woods Hole, Massachusetts.

PAPERS IN PHYSICAL OCEANOGRAPHY AND METEOROLOGY

PUBLISHED BY

MASSACHUSETTS INSTITUTE OF TECHNOLOGY

AND

WOODS HOLE OCEANOGRAPHIC INSTITUTION

VOL. XI, NO. 4

THE ANALYSIS OF TIDAL PHENOMENA IN NARROW EMBAYMENTS

BY

ALFRED C. REDFIELD

Contribution No. 529 from the Woods Hole Oceanographic Institution

and the

Oceanographic Laboratories, University of Washington

CAMBRIDGE AND WOODS HOLE, MASSACHUSETTS

JULY, 1950

CONTENTS

ACKNOWLEDGMENTS

This study was initiated while the author occupied the Walker Ames Professorship at the University of Washington.

The particular form of the mathematical treatment of the theory of reflected waves undergoing damping presented in this paper was developed by Mr. Henry Stommel of the Woods Hole Oceanographic Institution.

INTRODUCTION

The tides of coastal embayments derive their energy from the ocean tides rather than from the direct action of lunar and solar gravitational forces. They are considered to be part of co-oscillating systems in which the period is determined by the tide in the outer sea, while the detailed character of the motion depends on the size and form of the enclosed basin (Defant, 1925; Doodson and Warburg, 1941).

In narrow basins of simple form in which the influence of the earth's rotation is small, the motions resemble standing waves. Ideally, such waves are characterized by the simultaneous rise and fall of level on either side of a nodal line at which no change in elevation takes place. The elevation at high water increases with distance from the nodal line and slack water coincides with high and low water.

The properties of tides due to standing waves may be deduced by assuming the motion to result from a primary progressive wave moving up the channel which undergoes complete reflection at a barrier. Mathematically, this situation may be treated as the interference of two identical progressive waves moving in opposite directions and so related that both waves are in phase at the barrier. This treatment of standing waves assumes the presence of total reflection, the absence of damping and the absence of effects of the earth's rotation. Since these conditions are not realized in natural tidal basins, the standing wave concept leads to oversimplification.

In coastal embayments the most striking departure from the expectations of the standing wave concept is the discrepancy between times of high water and slack water, which may be great near the mouths of the larger bays and sounds. High water does not occur simultaneously within such enclosures but is earlier near the sea. Commonly, the nodal line is represented merely by a region in which the tidal range is small. These are effects which can be explained if damping of the primary and reflected waves by frictional or other effects is taken into account.

According to these concepts, the problem of tidal behavior in embayments is to determine numerically the properties of the primary and reflected waves so as to account for the observed relations of amplitude and stream velocity of the actual tide and to correlate these numerical properties with the geographical form of the embayment. In the present paper an attempt is made to treat the tidal behavior in such a way that the observed changes in elevation and motion of the water along the path of the wave may be used to determine the distribution of phase of the primary and reflected waves along the channel and to measure the damping.

The relations between the several aspects of a wave as it advances along a channel of uniform depth and width have been developed theoretically so as to show the times of high water and slack water, the range of the tide, and the phase relations of the primary and reflected waves along the channel for any degree of damping. By expressing the relationship of the several aspects of a reflected wave in a form in which the wave period is taken as the unit of time and distance is given in terms of the related phase changes, it is possible to eliminate the purely geographical dimensions and to obtain a wholly general description of the tide which may be used to indicate how any given channel distorts the behavior of the wave as it advances.

In the case of irregular channels, in order to justify the application of relations deduced for uniform channels, in which the change in phase of the primary and reflected

waves and their damping is proportional to the distance traveled and in which the velocity of the waves is constant, it is necessary to make the following assumptions:

1. That the effect of irregularities in cross section is to alter the velocity of the primary and reflected waves; i.e., to distort the geographical distribution of phase differences.
2. That damping is proportional to the phase change in the waves rather than to the distance traveled.
3. That the damping coefficient, as defined, is constant along the length of the channel.

THEORY OF REFLECTED WAVES UNDERGOING DAMPING

The theory of tidal waves in closed channels was fully developed on the analytical side by Airy (1845) from whose formulae those used in this paper are readily derived. Ferrel (1874) also investigated the effects of damping. More recently Fjeldstad (1929) has considered the theory of a free wave undergoing damping as it advances upon a coast from which it is reflected. The theoretical treatment presented by Fjeldstad has been reformulated with the considerations set forth below in mind.

In an embayment, tidal data are commonly obtainable from positions near the head where reflection may be considered to take place. From these positions the wave may be traced back seaward for distances which depend wholly on accidents of geography. Consequently, it is desirable to employ a treatment which starts at the point of reflection and measures time and distance from there, eliminating any explicit consideration of the wave at places where observations cannot be obtained. Motion of the water in a direction at right angles to the axis is ignored since the tidal movements in all but the wider embayments are reversing rather than rotatory.

The theory as developed should apply only to relatively narrow embayments of simple form. No account is taken of effects due to lateral forces arising from the rotation of the earth, to reflection at points along the channel, to the divergence of waves in branching channels, or to their convergence around islands. These effects appear as anomalies in the behavior of the observed tide as compared to theory.

The theory treats the tide as a single cosine wave. It may be applied rigorously only to one tidal component at a time. Where a single component dominates the tidal behavior it may be applied usefully to the data for the mean range and epoch of the actual tide.

The actual tide may be considered to be due to two progressive waves of like period traveling in opposite directions. One of these is the primary wave originating in the open sea. The other is the reflected wave originating at the barrier. At the barrier the two waves are equal in elevation and phase.

In a uniform channel the elevation of the primary wave is given by

$$\eta_1 = A \cos (\sigma t - kx)\ \epsilon^{-\mu x} \qquad (1)$$

that of the reflected wave by

$$\eta_2 = A \cos (\sigma t + kx)\ \epsilon^{\mu x} \qquad (2)$$

A is the amplitude of each of the waves at the barrier. σ is the change in phase per unit of time, and t is the time measured from the time of high water at the barrier, when $t = 0$. k is the change in phase per unit of distance, and x is the distance measured from the barrier, where $x = 0$. μ is the damping coefficient.

In order to give the treatment the generality required to describe the behavior of a wave of any period and length, it is convenient to employ the wave period as the unit of time. Time, t, is a fraction or multiple of the period and σ is a constant having the value of 360° per period. The time angle, σt, expresses the phase change in degrees during the lapse of time measured from high water at the barrier. σt_H will be used to denote the time angle when it is high water at any local point along the channel. Its value is numerically equal to the difference between the Greenwich epoch of the tide at the local point and at the barrier. The actual time difference is given by σt_H x wave period/360°.

Similarly, σt_S will denote the local time angle of slack water relative to high water at the barrier.

When the treatment is applied to channels of varying cross section, the wave length cannot be treated as a constant since the velocity of the wave may change from place to place. However, k may be defined as a phase difference of 360° and kx as the phase difference, relative to the barrier, due to position. Consequently, x denotes the part of a cycle which the wave will complete in passing between any point and the barrier.

In channels of uniform section, damping is usually related to the distance traversed by the wave. For channels of varying section, however, damping is assumed to be related to the phase change along the channel. Consequently $\epsilon^{-\mu x}$ represents the attenuation of the primary or reflected wave in the course of a fraction or multiple of a cycle, x.

To find the time of high water at any point.

The elevation of the water, η, at any time and place along the channel is given by

$$\eta = \eta_1 + \eta_2 \text{ or}$$

$$\eta = A\,[\cos(\sigma t - kx)\,\epsilon^{-\mu x} + \cos(\sigma t + kx)\,\epsilon^{\mu x}] \tag{3}$$

High water occurs when $\delta\eta/\delta t = 0$

or when

$$\sin(\sigma t - kx)\,\epsilon^{-\mu x} + \sin(\sigma t + kx)\,\epsilon^{\mu x} = 0$$

from which it follows that

$$\sin\sigma t\cos kx\,(\epsilon^{-\mu x} + \epsilon^{\mu x}) + \cos\sigma t\sin kx\,(\epsilon^{\mu x} - \epsilon^{-\mu x}) = 0$$

hence, letting σt_H denote the local time angle of high water,

$$\sigma t_H = \tan^{-1}(-\tan kx\tanh\mu x) \tag{4}$$

This function gives the time of high water at any position along the channel for any chosen coefficient of damping and is illustrated in Figure 1.

To find the relative heights of high water at any point.

It is useful to express the height of high water at any point along the channel by its ratio to the height at the reflecting barrier.

From (3) the elevation at any time and place may be written

$$\eta = 2A\,[\cos\sigma t\cos kx\cosh\mu x - \sin\sigma t\sin kx\sinh\mu x]$$

At high water it follows from (4) that

$$\cos\sigma t_H = \frac{1}{\sqrt{1 + \tan^2 kx\tanh^2\mu x}} \quad \text{and}$$

$$\sin\sigma t_H = \frac{-\tan kx\tanh\mu x}{\sqrt{1 + \tan^2 kx\tanh^2\mu x}}, \text{ consequently}$$

$$\eta/\eta_0 = 2A\,\frac{\cos kx\cosh\mu x + \tan kx\tanh\mu x\sin kx\sinh\mu x}{\sqrt{1 + \tan^2 kx\tanh^2\mu x}}$$

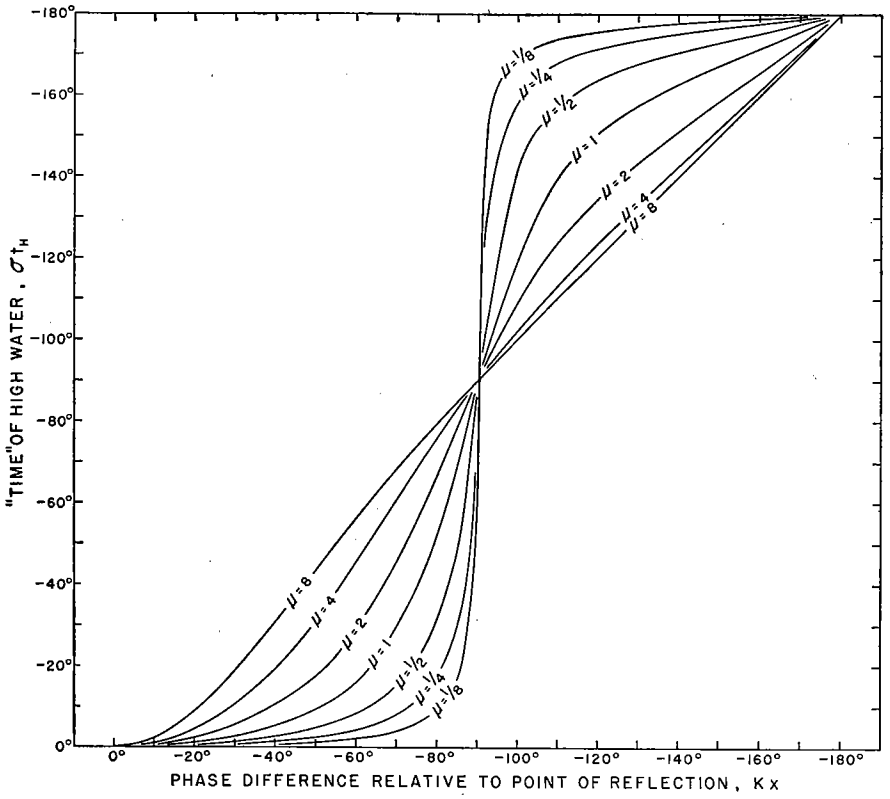

FIG. 1. Relations between time angle of high water, σt_H, and the phase difference of a primary wave along a channel, kx, for different coefficients of damping, μ, when reflection occurs at a barrier where $kx = 0$. See equation 4.

$$= 2A\sqrt{\cos^2 kx \cosh^2 \mu x + \sin^2 kx \sinh^2 \mu x}$$

$$= 2A\sqrt{\cos^2 kx + \cosh^2 \mu x - 1}$$

$$= 2A\sqrt{\tfrac{1}{2}(\cosh 2\mu x + \cos 2kx)}$$

The elevation at the barrier where $x = 0$ at high water is

$$\eta_0 = 2A$$

Restricting η and η_0 to the elevations at high water, the ratio

$$\eta/\eta_0 = \sqrt{\tfrac{1}{2}(\cosh 2\mu x + \cos 2kx)} \qquad (5)$$

This function relates the height of high water at any position along the channel to the height at the barrier for any chosen coefficient of damping, and is illustrated in Figure 2.

To find the time of slack water or maximum current at any point.

The velocity of the current due to the primary and reflected waves respectively at any time and place is given by

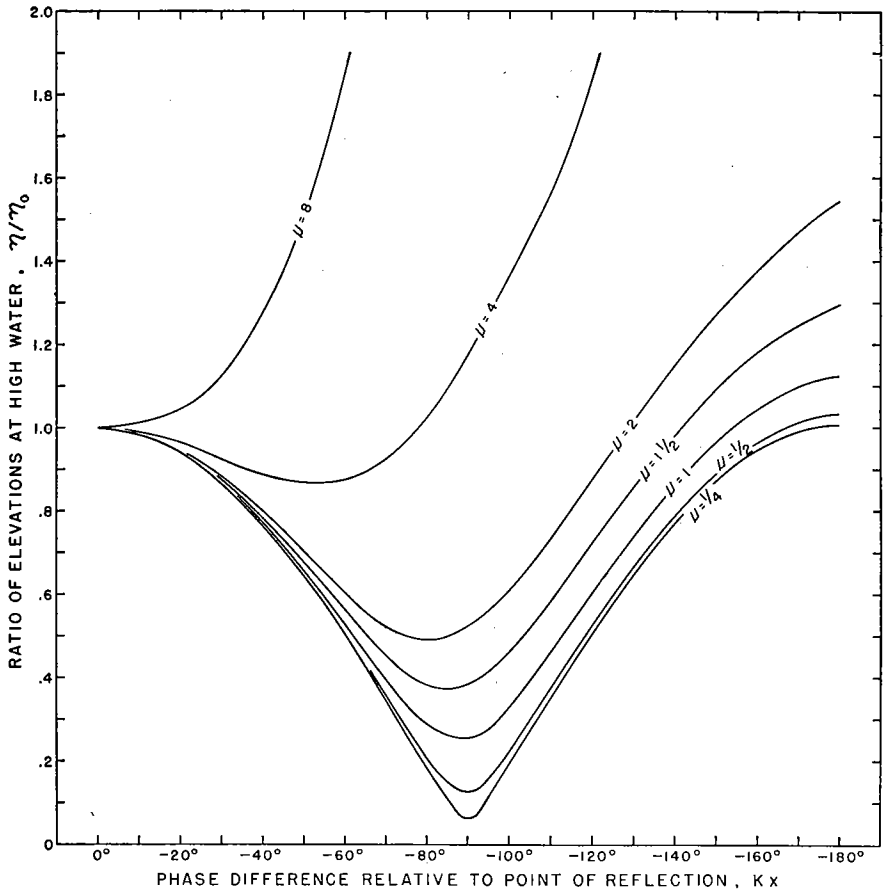

FIG. 2. Relations between the ratio of the height of high water, η, at any point along the channel to the height of high water at the reflecting barrier, η_0, and the phase difference between these points, kx, for different coefficients of damping, μ. Reflection occurs where $kx = 0$. See equation 5.

$$u_1 = A\frac{\sigma}{h}\left(\frac{1}{\sqrt{\mu^2 + k^2}}\right)\epsilon^{-\mu x}\cos(\sigma t - kx + \alpha) \text{ and} \tag{6}$$

$$u_2 = -A\frac{\sigma}{h}\left(\frac{1}{\sqrt{\mu^2 + k^2}}\right)\epsilon^{\mu x}\cos(\sigma t + kx + \alpha) \tag{7}$$

where h is the depth and $\alpha = \tan^{-1}\frac{\mu}{k}$. α represents the phase difference between the time of high water and maximum current in a progressive wave undergoing damping. The velocity of the resulting tidal stream is given by $u = u_1 + u_2$ and slack water occurs when $u_1 + u_2 = 0$.

At the barrier, where $x = 0$, $u_1 + u_2 = 0$ at all values of t and it is always slack water. At any other point along the channel $u_1 + u_2 = 0$ and slack water occurs when

$$\epsilon^{-\mu x}\cos(\sigma t - kx + \alpha) - \epsilon^{\mu x}\cos(\sigma t + kx + \alpha) = 0 \tag{8}$$

$$\cos(\sigma t - kx + \alpha) = \cos(\sigma t + \alpha)\cos kx + \sin(\sigma t + \alpha)\sin kx$$

$$\cos(\sigma t + kx + \alpha) = \cos(\sigma t + \alpha)\cos kx - \sin(\sigma t + \alpha)\sin kx$$

$$\cos(\sigma t + \alpha)\left[\epsilon^{-\mu x}\cos kx - \epsilon^{\mu x}\cos kx\right] + \sin(\sigma t + \alpha)\left[\epsilon^{-\mu x}\sin kx + \epsilon^{\mu x}\sin kx\right] = 0$$

$$\cos(\sigma t + \alpha)\cos kx \sinh \mu x - \sin(\sigma t + \alpha)\sin kx \cosh \mu x = 0$$

$$\tan(\sigma t + \alpha) = \frac{\tanh \mu x}{\tan kx} \tag{9a}$$

Letting σt_S denote the local time angle of slack water

$$\sigma t_S = \tan^{-1}\left(\frac{\tanh \mu x}{\tan kx}\right) - \alpha \tag{9b}$$

This function relates slack water to the phase difference due to position along the channel for any chosen coefficient of damping and is illustrated in Figure 3.

The maximum current will precede or follow slack water by one quarter period or 90°.

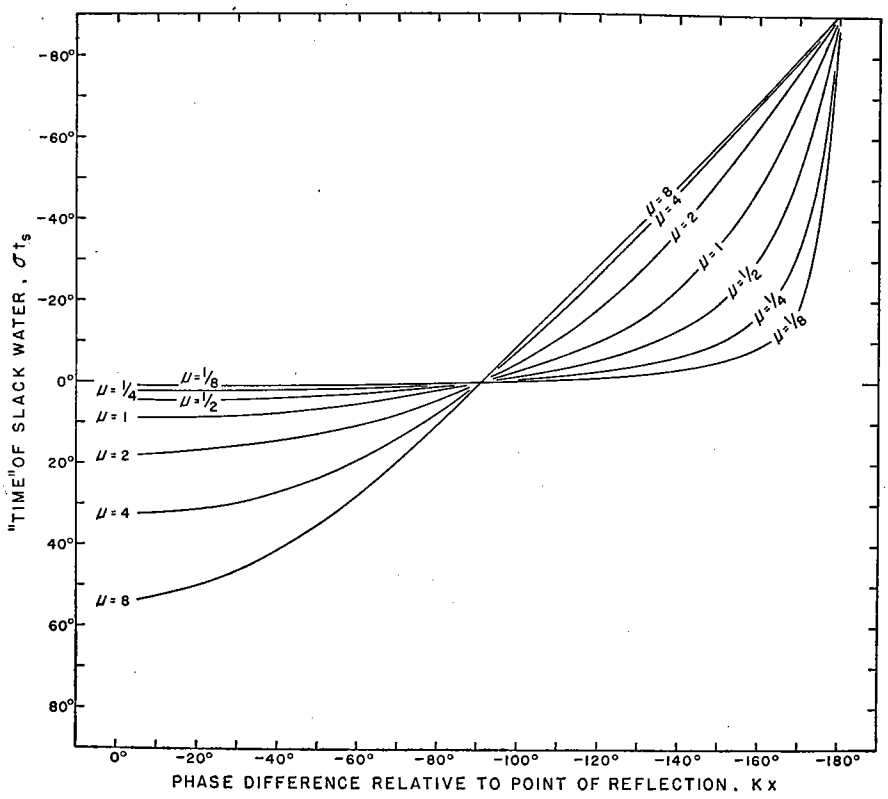

FIG. 3. Relations between the time angle of slack water, σt_s, and the phase difference of a primary wave along a channel, kx, and the coefficient of damping, μ, when reflection occurs at a barrier where $kx = 0$. See equation 9b.

Application.

Tidal data are available in the form of records of the time of high water, the elevation at high water and the time of slack water or maximum current at various positions along the channels. In order to obtain an indication of the effect of a given channel on the

primary or reflected wave, information on the distribution of phase differences along the channel and on the damping is required.

By combining the relations defined by equations (4) and (5) or Figures 1 and 2, Figure 4 was constructed in which the observed variables (the ratio of the high water elevations, η/η_0, and the local time angle of high water, σt_H, are represented by the rectangular coordinates and the desired properties of the primary wave (the phase relations and the coefficient of damping) are represented each by a series of curves. This nomogram is completely general being independent of the actual dimensions of the basin or of the period of the wave. By choosing a logarithmic scale to represent the ratio of the elevations, η/η_0, the shape of the curves remains unchanged when the ordinates are multiplied by any number. It is consequently a simple matter to plot a series of tidal data giving the elevations and time of high water, expressed as Greenwich epochs, on a similar semi-logarithmic coordinate system and by superposing the curves of Figure 4 to determine whether a satisfactory fit can be obtained.

If a satisfactory fit can be obtained, the properties of the primary wave as determined

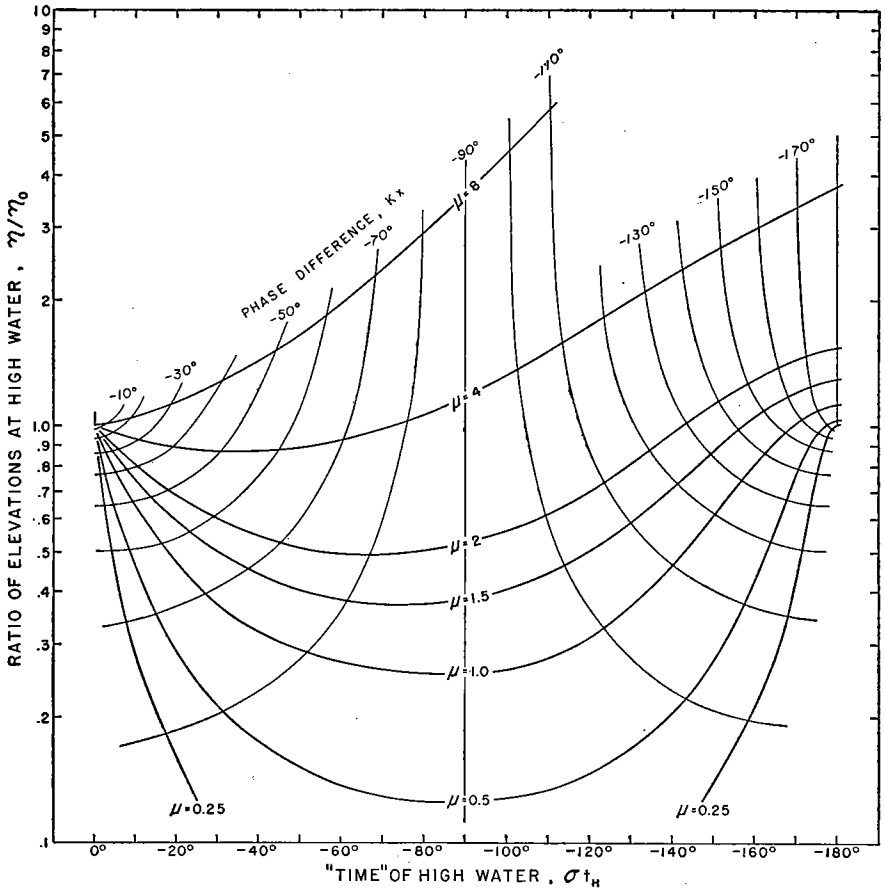

FIG. 4. Relations between the ratio of height of high water at any point to the height of high water at the barrier, η/η_0, the time angle of high water, σt_H, the phase difference of a primary wave at that point relative to the barrier, kx, and the coefficient of damping, μ. Reflection occurs where $\eta/\eta_0 = 1.0$ and $\sigma t_H = 0$.

by the position of the points on the nomogram may be transferred to charts or diagrams in which the geographical position of the points are indicated and these may be used to determine the distribution of phase differences of the primary wave in the channel. These phase differences, with change of sign, will also apply to the reflected wave.

In an entirely similar way, the relations of equations (4) and (9b), (Figures 1 and 3d), may be combined to construct a graph in which the local time angle of high water, σt_H, is related to that of slack water, σt_S, as in Figure 5. This figure may be used to check the adequacy of the theoretical treatment and to predict the expected time of slack water from data for the time of high water.

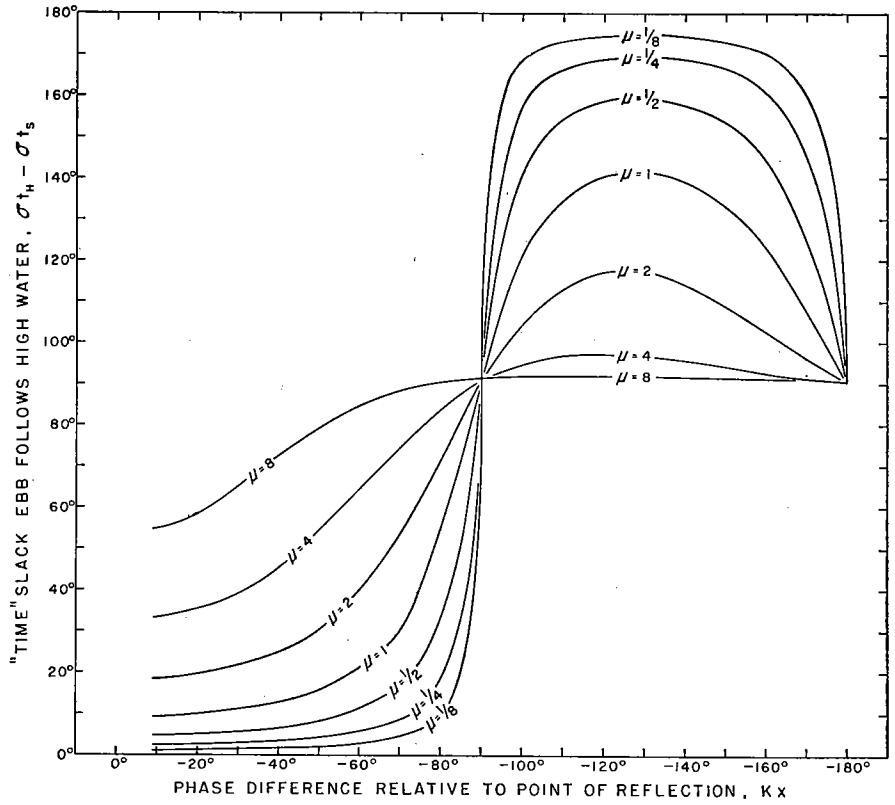

FIG. 5. Relations of the time angle between high water, σt_H, and slack water, σt_S, at any point along a channel, the phase difference of a primary wave at that point relative to the barrier, kx, and the coefficient of damping, μ, when reflection occurs at a barrier where $kx = 0$.

ANALYSES OF REAL TIDAL SYSTEMS

The utility of the foregoing method of analysis has been tested by application to three large embayments, Long Island Sound, the Bay of Fundy and the system formed by the Strait of Juan de Fuca and the Strait of Georgia. The two former, which have been cited as examples of typical standing wave systems, were selected because of their relatively regular configuration. In contrast, the Juan de Fuca-Georgia system presents great topographical complexity and the tidal phenomena in the outer strait depart widely from those of typical standing waves. The existence there of well marked mixed tides also permits the behavior of components of different period to be examined in the same basin. It was interest in this system, which does not appear to have been examined in detail, which led to the present study. These systems have been discussed by Harris (1898–1907) and Marmer (1926).

For Long Island Sound and the Bay of Fundy data given in the Tide Tables and Current Tables issued by the U. S. Coast and Geodetic Survey (1947, 1948) have been employed. Since in the North Atlantic the tidal phenomena are dominated by the M_2 component, it has been assumed that the tabulated values for mean range, high water interval, and flood interval, could be taken to represent the behavior of a single wave having a speed number of 29° per hour. This assumption is justified by Proudman and Doodson (1924).

On the Pacific coast where the tides are of the mixed type, it is desirable to employ analyzed data for the principal components. Fortunately such data are available from twelve stations distributed along the Juan de Fuca-Georgia Straits system (see Figure 11). These data were supplied by the Coast and Geodetic Survey through the kindness of Dr. Marmer and amplified the information available in published form (Coast and Geodetic Survey, 1942).

In examining the success with which the deduced relations correlate the observations on range and time of high water along a channel, it may be expected, if the realities of geography or factors not considered by the theory do not produce anomalous effects, that the observed data will fall among one of the lines characteristic of the damping coefficient when plotted on the coordinate system of Figure 4. If so, the phase relations may be read off the graph.

It is to be anticipated that individual points of observation will show departures from the general expectancy for the behavior of the wave along the main channel, because tide gauges are frequently installed in minor embayments in which purely local conditions influence the small offshoot waves which are actually measured.

The Long Island Sound System.

The analysis is shown in Figure 6 in which the data for mean range of tide and Greenwich epoch, G, for the stations listed in Table I are plotted on the coordinate system of Figure 4. The position of these stations is shown in Figure 7. The best fit of the data to the coordinate system is obtained by assuming that reflection occurs from a region extending from Eatons Point to Glen Cove and including Great Captain Island (Stations 30–32) where the mean tidal range is maximal at 7.2 to 7.4 feet. East of Eatons Point, the range of tide decreases as the time of high water becomes earlier. The observations made within Long Island Sound proper, along the south side of Block

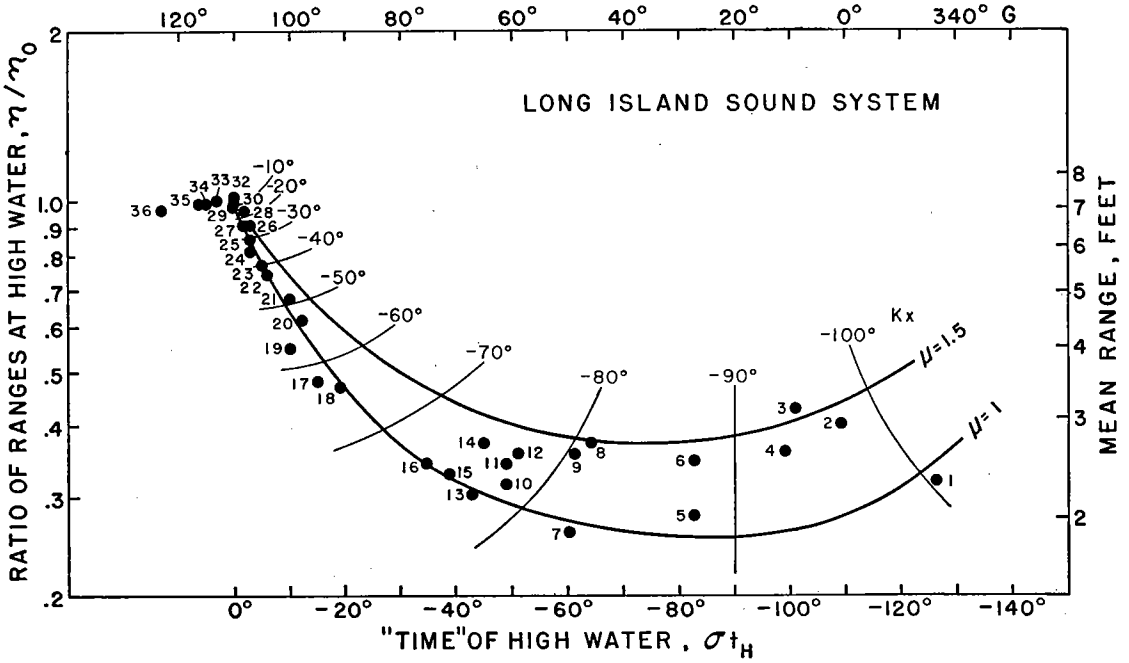

FIG. 6. Analysis of the Long Island Sound System. To identify the points see Table I.

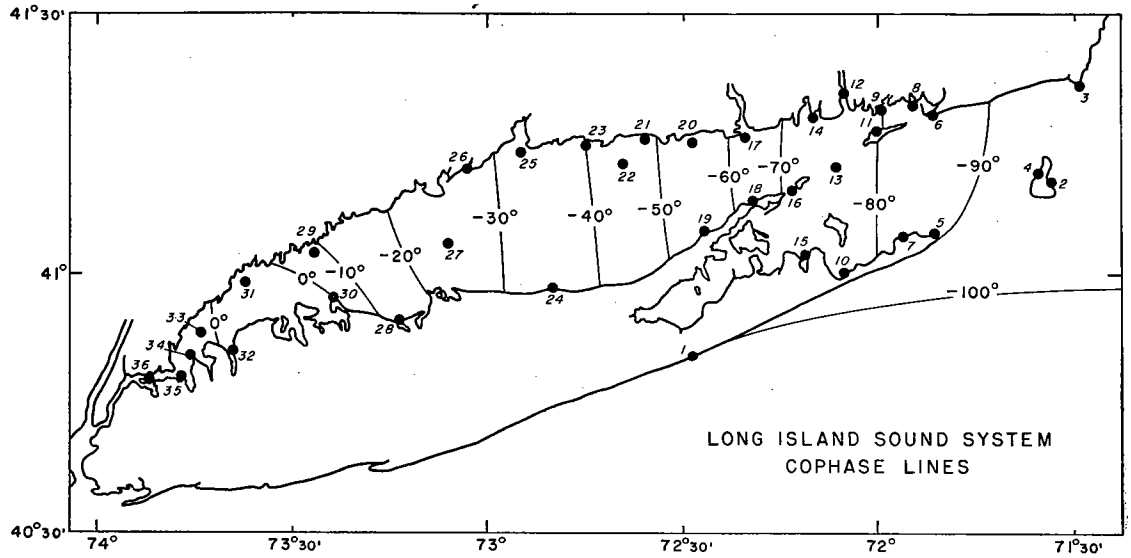

FIG. 7. Chart of Long Island Sound showing stations and cophase lines. To identify the stations see Table I.

Island Sound, and including a station on the outer coast of Long Island at Shinnecock Inlet (Station 1) fall closely along the coordinate for the damping coefficient $\mu = 1.0$.

The phase differences of the primary wave at each station relative to the point of reflection may be determined from Figure 6 and are entered in Table I. From these

TABLE I

TIDAL DATA FOR LONG ISLAND SOUND SYSTEM

No.	Station	Lat.	Long.	High Water Interval hours	G degrees	Mean Range feet	kx degrees
1	Shinnecock Inlet	40° 50′	72° 29′	6.92	343	2.3	— 101
2	Block Island Harbor	41° 10′	71° 33′	7.50	0	2.9	— 97
3	Point Judith	41° 22′	71° 29′	7.75	8	3.1	— 94
4	Block Island Pond	41° 11′	71° 35′	7.82	10	2.6	— 93
5	Montauk Point	41° 04′	71° 52′	8.33	26	2.0	— 88
6	Watch Hill Point	41° 18′	71° 52′	8.32	26	2.5	— 87
7	Montauk Harbor	41° 04′	71° 56′	9.12	49	1.9	— 82
8	Stonington	41° 20′	71° 54′	8.98	45	2.7	— 81
9	Noank	41° 19′	71° 59′	9.08	48	2.6	— 81
10	Promised Land	41° 00′	72° 05′	9.30	60	2.3	— 78
11	West Harbor, Fishers Isl.	41° 16′	72° 00′	9.52	60	2.5	— 77
12	New London	41° 22′	72° 06′	9.43	58	2.6	— 77
13	Little Gull Island	41° 12′	72° 06′	9.72	66	2.2	— 77
14	Millstone Point	41° 18′	72° 10′	9.65	64	2.7	— 75
15	Three Mile Harbor	41° 02′	72° 11′	9.87	70	2.4	— 75
16	Plum Gut Harbor	41° 10′	72° 12′	10.00	74	2.5	— 73
17	Saybrook Jetty	41° 16′	72° 21′	10.66	94	3.5	— 53
18	Truman Beach	41° 08′	72° 19′	10.50	90	3.4	— 63
19	Horton Point	41° 05′	72° 27′	10.85	99	4.0	— 56
20	Duck Island	41° 15′	72° 29′	10.77	97	4.5	— 53
21	Madison	41° 16′	72° 36′	10.83	99	4.9	— 49
22	Falkner Island	41° 13′	72° 39′	10.95	103	5.4	— 42
23	Money Island	41° 15′	72° 45′	10.98	104	5.6	— 40
24	Herod Point	40° 58′	72° 50′	11.03	106	5.9	— 36
25	New Haven Harbor	41° 14′	72° 55′	11.02	106	6.2	— 31
26	Millford	41° 13′	73° 03′	11.03	106	6.6	— 25
27	Stratford Shoal	41° 04′	73° 06′	11.05	107	6.6	— 25
28	Nissequoque River	40° 54′	73° 14′	11.08	107	7.0	— 17
29	Greens Ledge	41° 03′	73° 27′	11.10	109	7.2	— 10
30	Eatons Point	40° 57′	73° 24′	11.12	109	7.2	0
31	Great Captain Island	40° 59′	73° 37′	11.12	109	7.3	0
32	Glen Cove	40° 52′	73° 39′	11.12	109	7.4	0
33	Execution Rocks	40° 53′	73° 44′	11.20	112	7.3	—
34	Hewett Point	40° 50′	73° 45′	11.25	114	7.2	—
35	Willetts Point	40° 48′	73° 47′	11.28	115	7.2	—
36	Hunts Point	40° 48′	73° 52′	11.50	122	7.0	—

values cophase lines[1] representing the advance of the primary wave into Long Island Sound have been drawn in Figure 7. The observations at Shinnecock Inlet where the phase difference is − 101° may be taken to represent conditions in the ocean as the wave approaches Block Island Sound. The ocean wave appears to approach the coast in a northerly direction, nearly normal to the general coastal trend, as judged by its time of arrival at Block Island and No Mans Land. The primary wave which produces the tide of Long Island Sound appears to pivot on Montauk Point to advance in a westerly direction. A line extending from Montauk Point northeasterly across Block Island Sound

[1] The term "cophase lines" is used to designate lines marking regions in which the phase of the primary (or reflected) wave is identical at any one time. This usage is intended to distinguish the description of these mathematically fictitious waves from that of the resultant real wave, conventionally described by cotidal lines.

marks the 90° phase difference, or ¼ cycle, from the point of reflection. Within Long Island Sound proper, between the Race and Eatons Point, the phase change of the primary wave is 75°.

Anomalous observations. In Figure 6, a number of stations appear where the range is greater than would be expected if the value of μ is 1.0. These stations lie along the northern shore of Block Island Sound and in Fishers Island Sound (Stations 3, 6, 8, 9, 11, 12). They include the stations on Block Island (Stations 2, 4) and extend into Long Island Sound only as far as Millstone Point, Connecticut (Station 14).

These observations show that the wave which advances westward across Block Island Sound is higher on its right-hand side, an effect which may be attributed to the rotation of the earth. It is probable also that the ocean wave entering the bight between Block Island and No Mans Land is undergoing augmentation by reflection from the coast. The effect of this also would be to increase the amplitude of the offshoot wave sweeping into Block Island Sound along those parts closest to the mainland.

Within Long Island Sound there is little indication that the range of tide is greater along the northern shore. The higher amplitudes observed in the wave traversing Fishers Island Sound do not extend much beyond Millstone Point, being absent at the mouth of the Connecticut River. Evidently the main features of the tide within Long Island Sound are determined by the wave which passes between Montauk Point and Block Island and enters the Sound through the Race.

The conditions west of Glen Cove are also anomalous. Between this station and Hunts Point (Station 36), the mean range of tide declines slightly while the time of high water is progressively later. These effects are evidently due to the escape of water from the Sound through the East River.

The velocity of the primary wave. By measuring the geographical distances along the mid-line of the Sound between the several cophase lines, the time course of the primary wave may be determined. The total distance, 90 miles, from Southwest Ledge to Great Captain Island is traversed in about 3.3 hours or at 27 knots. The velocity is practically uniform at this rate between Cornfield Point Lightship and the western end of the Sound. Between the lightship and the Race the velocity is lower—about 20 knots—while in Block Island Sound it appears to be higher, about 32 knots, though there the positions of the cophase lines are not as precisely defined.

The time of slack water. Current data are available from about twenty stations located so that the time of high water can be ascertained from nearby points. These are listed in Table II. A value for the phase difference, kx, of the incoming wave relative to the point of reflection has been assigned to each station and the corresponding value of $\sigma t_H - \sigma t_S$, the time angle between high and slack water has been found from Figure 5, assuming a damping coefficient, μ, equal to 1.0. The actual time angle $G_S - G_H$, has also been estimated from the Greenwich epochs of the flood interval at the current station and of high water at the nearby tidal station. The comparison between the observed and estimated interval is shown in Figure 8.

The time of slack water relative to high water agrees in its general trend with that predicted in theory, particularly in those points situated in Block Island Sound and the Race. Within Long Island Sound a number of points deviate from the expectancy but quite unsystematically. These deviations are due to irregularities in the local time of slack water, rather than to that of high water, along the length of the Sound.

TABLE II

PHASE DIFFERENCE BETWEEN HIGH WATER AND SLACK WATER IN LONG ISLAND SOUND SYSTEM

Current Station	Reference Stations for High Water	Phase difference of inflowing wave[1]	Time angle between High Water and Slack Water		Difference
			from theory[2]	from tidal data	
		kx	$(\sigma t_H - \sigma t_S)$	$G_S - G_H$	
South West Ledge	Block Island Pond	— 93°	102°	100°	+ 2°
Montauk Point	Montauk Point	— 88°	82°	49°	+ 33°
North of Block Island—4 Miles	Block Island Pond	— 93°	102°	114°	— 12°
Between Shagway Reef and Cerebus Shoal	Montauk Point	— 82°	65°	57°	+ 8°
3 Miles N. E. of Gardners Island	Promised Land	— 78°	49°	41°	+ 8°
Ram Island Reef	Noank	— 80°	55°	48°	+ 7°
The Race near Valiant Rock	Little Gull Island	— 78°	49°	55°	— 6°
Between Great Gull Island and Plum Island	Little Gull Island	— 76°	43°	35°	+ 8°
Plum Gut	Plum Gut Harbor	— 73°	36°	13°	+ 23°
Bartlett Reef	Millstone Point	— 74°	38°	15°	+ 23°
Cornfield Point Lightship	Truman Beach	— 61°	22°	19°	+ 3°
Off Terry Point	Truman Beach	— 63°	23°	27°	— 4°
Off Kelsey Point	Duck Island	— 52°	17°	—17°	+ 34°
6 Miles S. of Sachem Head	Falkner Island	— 42°	13°	27°	— 14°
1 Mile S. of Sachem Head	Falkner Island	— 42°	13°	2°	+ 11°
1 Mile S. of Roanoke Point	Falkner Island	— 40°	13°	26°	— 13°
2 Miles N. E. of Oldfield Point	Stratford Shoal	— 25°	11°	16°	— 5°
Off Point No Point	Stratford Shoal	— 23°	10°	10°	0
Off Crane Neck Point	Nissequoque River	— 19°	10°	8°	+ 2°
½ Mile N. of Eatons Point	Eatons Point	0	0	— 12°	+ 12°
¾ Mile N. of Lloyd Point	Glen Cove	0	0	5°	— 5°

[1] Phase at current station relative to point of reflection.

[2] Estimated assuming damping coefficient, μ, equal to 1.0.

Summary. The Long Island Sound tidal system conforms satisfactorily to theoretical expectation along a stretch extending from the outer coast of Long Island, across the southern half of Block Island Sound, and up Long Island Sound to a point of reflection at the longitudes of Eatons Point and Glen Cove. The damping coefficient of this system is about 1.0; the velocity of the primary wave is about 27 knots. The properties of the wave may be traced seaward through a phase difference of 101°. A line extending from Montauk Point northeasterly lies one-quarter wave length from the point of reflection.

Anomalous behavior attributable to the tidal flow through East River is observed west of Glen Cove. The amplitude of the tidal wave is also augmented beyond expectation along the north side of Block Island Sound and in Fishers Island Sound, but this portion of the primary wave does not penetrate into Long Island Sound sufficiently to produce disturbing effects.

The analysis appears to be adequate to account for the properties of a system which

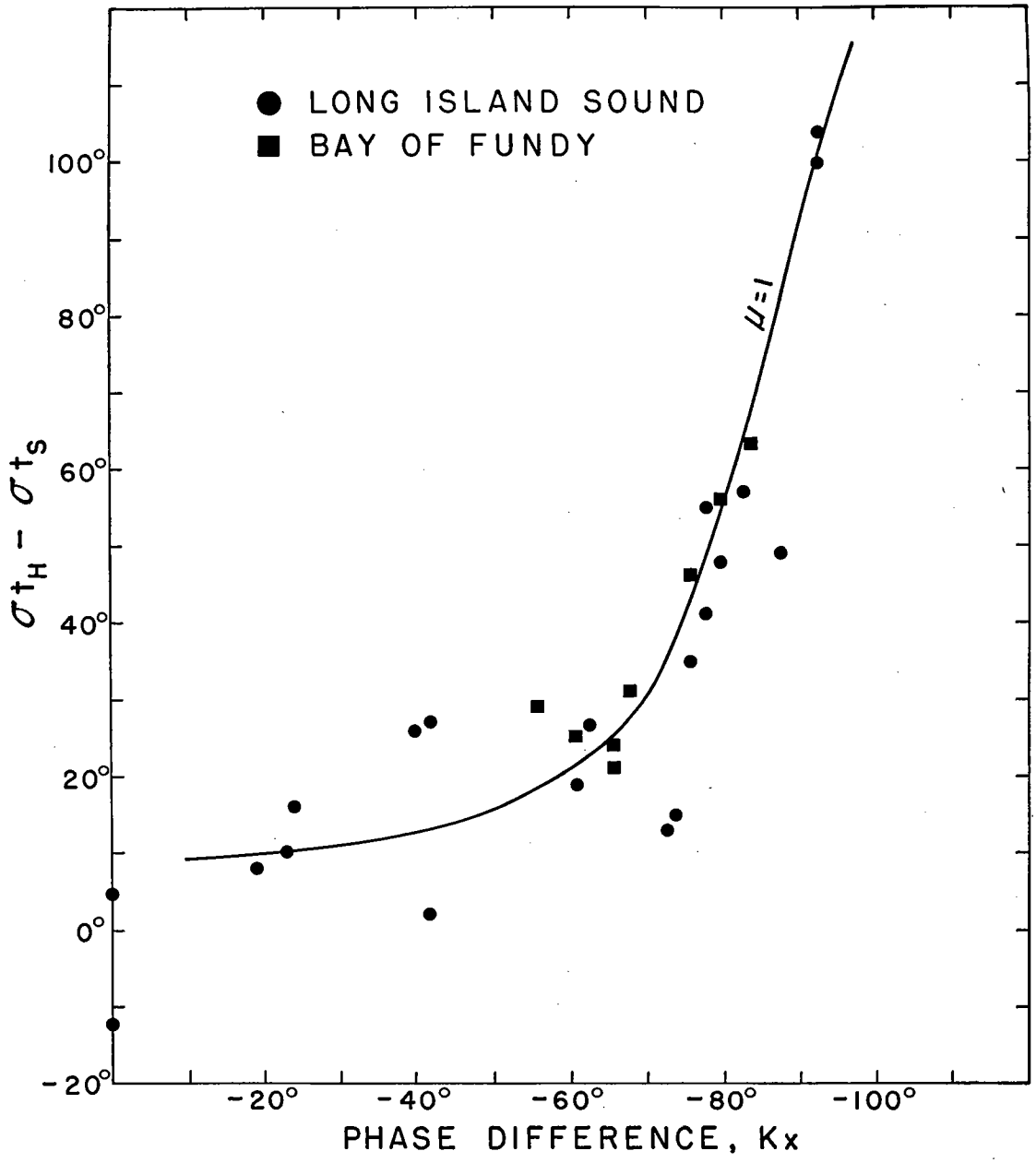

FIG. 8. Comparison of the recorded time angles between slack water and high water, $G_S - G_H$, which are shown by points and the time angles, $\sigma t_H - \sigma t_S$, deduced assuming a damping coefficient, μ, equal to 1.0. See Table II and Table V. Data from Long Island Sound and the Bay of Fundy.

has been described as an example of the standing wave type of tidal motion. The introduction of the quantitative consideration of damping has, however, permitted the characteristics of the phenomena which depart from those of an ideal standing wave to receive a rational interpretation.

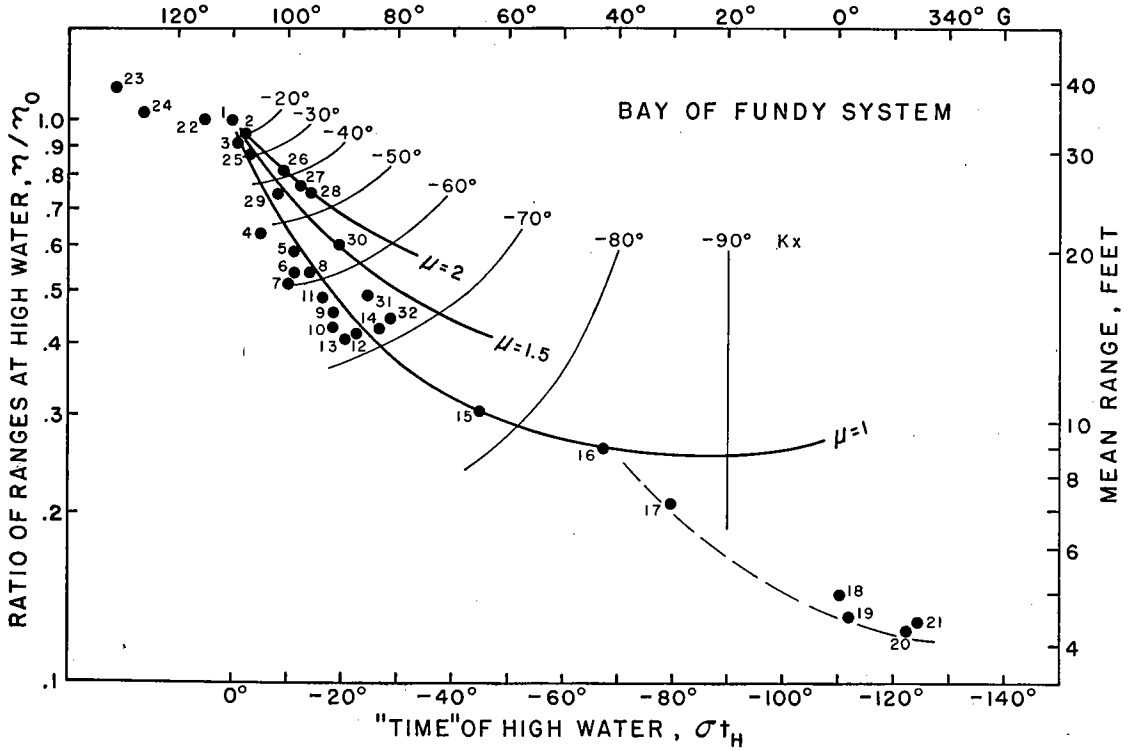

FIG. 9. Analysis of the Bay of Fundy system. To identify the points see Table III.

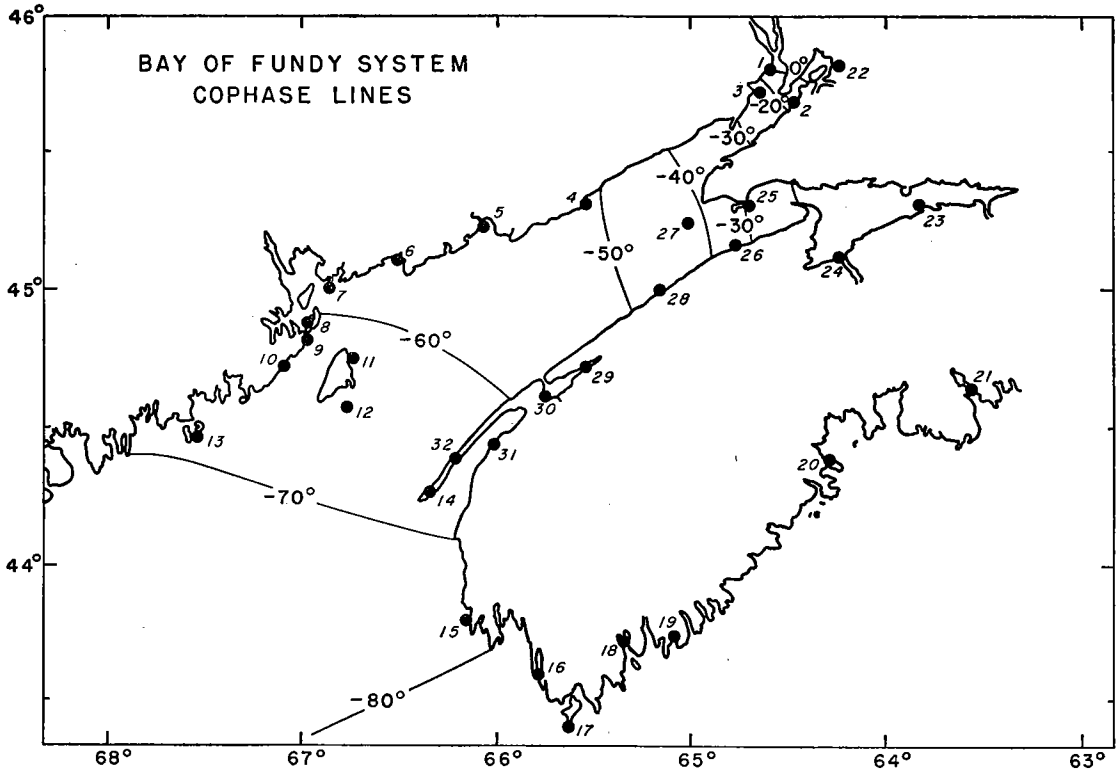

FIG. 10. Chart of the Bay of Fundy showing stations and cophase lines. To identify the stations see Table III.

TABLE III

TIDAL DATA FOR BAY OF FUNDY SYSTEM

No.	Station	Lat.	Long.	High Water Interval G hours	G degrees	Mean Range feet	kx degrees
1	Hopewell Cape	45° 52′	64° 34′	11.76	110	34.3	0
2	Joggins	45° 41′	64° 28′	11.68	108	32.7	−18
3	Grindstone Island	45° 43′	64° 37′	11.70	109	31.4	−22
4	Quaco	45° 20′	65° 32′	11.50	105	22.1	−51
5	St. John	45° 15′	66° 04′	11.28	99	20.1	−55
6	Lepreau Bay	45° 07′	66° 29′	11.23	99	18.5	−58
7	L'Etang Harbor	45° 02′	66° 49′	11.25	100	17.7	−59
8	Welchpool	44° 53′	66° 57′	11.10	96	18.3	−58
9	West Quoddy Head	44° 49′	66° 59′	10.97	92	15.7	−64
10	Moose Cove	44° 44′	67° 07′	10.96	92	14.8	−66
11	No. Head—Grand Manan	44° 46′	66° 45′	11.03	94	16.7	−62
12	Three Islands	44° 35′	66° 46′	11.82	88	14.4	−67
13	Moose Peak Light	44° 39′	67° 13′	10.93	90	13.9	−67
14	Grand Passage — St. Marys Bay	44° 16′	66° 20′	10.75	84	14.7	−68
15	Yarmouth	43° 48′	66° 08′	10.15	66	10.5	−78
16	Lower East Pubnico	43° 38′	65° 47′	9.37	44	9.0	−84
17	Cape Sable	43° 26′	65° 38′	9.02	32	7.0	–
18	Shelburne	43° 45′	65° 20′	8.05	4	5.0	–
19	Lockport	43° 44′	65° 05′	7.95	0	4.6	–
20	Lunenburg	44° 20′	64° 18′	7.65	350	4.3	–
21	Halifax	44° 40′	63° 34′	7.62	348	4.4	–
22	Amherst	45° 50′	64° 13′	11.95	115	34.5	–
23	Burntcoat Head	45° 18′	63° 49′	0.15	131	39.4	–
24	Horton Bluff	45° 06′	64° 13′	12.36	126	35.9	–
25	Spencer Island	45° 20′	64° 42′	11.65	107	29.9	−29
26	Black Rock	45° 10′	64° 46′	11.41	101	27.6	−39
27	Isle Haute	45° 15′	65° 00′	11.31	98	26.3	−43
28	Port George	45° 01′	65° 10′	11.25	96	25.3	−46
29	Annapolis	44° 45′	65° 30′	11.41	102	21.7	−44
30	Digby Pier	44° 38′	65° 45′	11.00	91	20.7	−56
31	Weymouth	44° 27′	66° 01′	10.85	86	17.3	−64
32	Petit Passage — St. Marys Bay	44° 24′	66° 13′	10.70	82	15.3	−68

The Bay of Fundy System.

The analysis is shown in Figure 9 in which the mean range of tide and the Greenwich epoch, G, for the stations listed in Table III are plotted in the coordinate system of Figure 4. The positions of these stations are shown in Figure 10. The best fit of the data to the coordinate system is obtained by assuming that reflection occurs near Hopewell Cape (Station 1) at the head of Chignecto Channel and from the neighborhood of Cape Split at the entrance to the Minas Basin (between Stations 24 and 25). Along the New Brunswick coast, in the Grand Manan region and along the southwest coast of Nova Scotia seaward as far as Lower East Pubnico (Station 16) the range of tide diminishes as high water comes earlier. The points scatter about or fall slightly below the curve representing the damping coefficient $\mu = 1.0$.

Following the Nova Scotia coast eastward from Cape Sable (Stations 17 to 21) the

range of tide continues to diminish and high water comes earlier. The points representing these features of the tide along the coast as far east as Halifax and beyond follow a different curve (indicated by a broken line in Figure 10). This is interpreted to mean that these stations on the outer coast are beyond the system dominated by reflection from the Bay of Fundy.

Along the eastern side of the Bay of Fundy (Stations 25 to 32) the range of tide is higher than would be expected if the value of μ is 1.0. This anomaly may be attributed to effects of the earth's rotation which is recognized to produce higher tides along the Nova Scotia side of the Bay (Marmer, 1926). In addition it seems possible that the tidal wave may be reflected earlier from the approaches to the Minas Basin than from Chignecto Channel; an effect which would also augment the range along the off-lying shores (Stations 26 to 28). Local conditions in the Annapolis Basin and in St. Marys Bay may also contribute to the anomalous ranges observed at Stations 28 to 32.

The conditions within Minas Basin and at Amherst (Stations 22 to 24) also appear anomalous, high water occurring later than is expected from the range. It is as though in these shallow channels the wave progresses more slowly and with much greater damping, and the volume of the reflected wave is insufficient to distort the relationships in the main system.

The phase relations of the primary wave in the Bay of Fundy are shown in Figure 10. They indicate that the portion of the wave which conforms to the analysis extends seaward a little over 80° from the head of the Bay. The wave progresses rapidly over the outer part of the Bay, but its progress is retarded as the water shoals at the inner end as shown by the closer spacing of the cophase lines. The estimated velocities of the primary wave as it crosses the several cophase lines, and the mean depth across the Bay at these positions is shown in Table IV.

TABLE IV

VELOCITY OF INFLOWING WAVE IN BAY OF FUNDY

Position relative to point of reflection kx	Velocity knots	Mean Depth fathoms	Position relative to point of reflection kx	Velocity knots	Mean Depth fathoms
$-70°$	145	58	$-40°$	54	17
$-60°$	128	53	$-30°$	41	17
$-50°$	84	30	$-20°$	23	8

The time of slack water. The phase difference between time of high water G_H and of slack water G_S has been estimated for a number of current stations within the Bay of Fundy and are entered in Table V. The agreement between this interval, as estimated from tide and current data, with that predicted theoretically using Figure 5 is excellent. The results are combined with those from Long Island Sound in Figure 8.

Summary. The Bay of Fundy tidal system conforms satisfactorily to the theoretical expectation along a stretch extending from Lower East Pubnico on the southwest coast of Nova Scotia to the head of the Chignecto Channel and the entrance to Minas Basin where the point of reflection appears to be situated. The phase change undergone by the primary wave between these limits is about 80°. The damping coefficient is about 1.0, as in the case of Long Island Sound.

The velocity of the primary wave is 145 knots in the outer part of the Bay but

TABLE V

PHASE DIFFERENCE BETWEEN HIGH WATER AND SLACK WATER IN BAY OF FUNDY SYSTEM

Current Station	Reference Station for High Water	Phase difference of inflowing wave[1]	Time angle between High Water and Slack Water		Difference
			from theory[2]	from tidal data	
		kx	$\sigma t_H - \sigma t_s$	$G_s - G_H$	
13 Miles S. W. of Seul Island	Lower East Pubnico	— 84°	68°	63°	+ 5°
17 Miles S. W. of Cape Fourchu	Yarmouth	— 80°	55°	56°	— 1°
10 Miles W. of Lurcher Shoal	Yarmouth	— 76°	43°	46°	— 3°
5 Miles W. of Brier Island	Grand Passage	— 68°	27°	31°	— 4°
5 miles S. E. of Gannet Rock	Three Islands	— 66°	23°	24°	— 1°
Grand Manan Channel	Moose Cove	— 66°	26°	21°	+ 5°
20 Miles W. of Prim Point	Lepreau Bay	— 61°	22°	25°	— 3°
20 miles S. of Cape Spencer	St. John	— 56°	19°	29°	+ 10°

[1] Phase at current station relative to point of reflection.
[2] Estimated assuming damping coefficient, μ, equal to 1.0.

diminishes with the depth of the water and is reduced to 23 knots within Chignecto Channel.

Anomalous behavior attributable to the rotation of the earth and to local conditions is observed along the west coast of Nova Scotia.

The Juan de Fuca and Georgia Straits System.

In the system of sounds extending from the mouth of the Strait of Juan de Fuca, through the passages of the San Juan Islands to the head of Georgia Strait, the tides are of the mixed type which permits comparison of the behavior of waves of different period in the same channel. The length of the system, in excess of 200 miles, is sufficient to require nearly five hours for the crest of high water to pass from the sea coast to the head of Georgia Strait.

The most striking special feature which requires explanation is the change along the channel of the relative values of the constants for the diurnal and semi-diurnal components of the tide. This leads to the almost complete suppression of the semi-diurnal wave in the neighborhood of Victoria where the tides are diurnal, or almost so, on an average of more than twenty days each month (Hydrographic and Map Service, 1940). The amplitudes of the K_1 and M_2 components and their ratios at several points are as follows:

	M_2	K_1	M_2/K_1
Neah Bay	2.67	1.60	1.67
Port Angeles	1.70	2.17	0.78
Victoria	1.21	2.07	0.58
Friday Harbor	1.83	2.49	0.73
Sand Heads	2.97	2.83	1.05
Whaleton	3.31	3.04	1.09

The ratios of the several diurnal components to one another remain constant along the channel, as do also the ratios of the semi-diurnal components so that the behavior of the M_2 and K_1 components may be taken as typical of the other components according to their species.

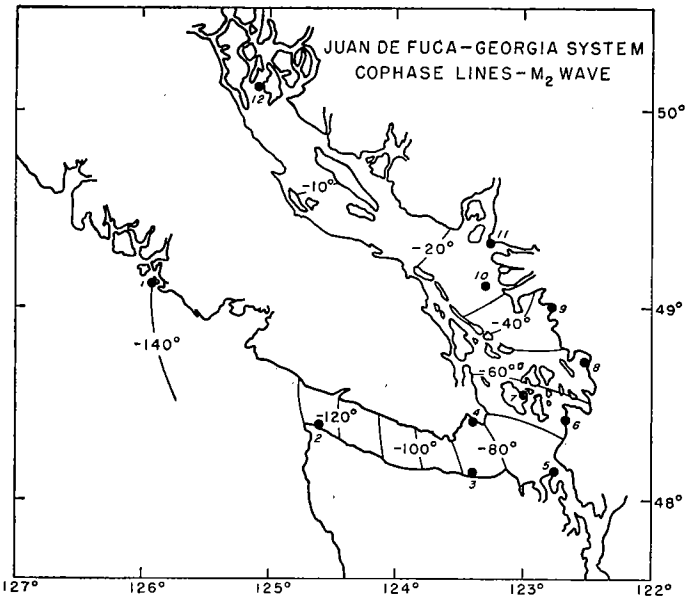

FIG. 11. Chart of the Juan de Fuca-Georgia Straits system showing stations and the cophase lines for the M_2 component. To identify the stations see Table VI.

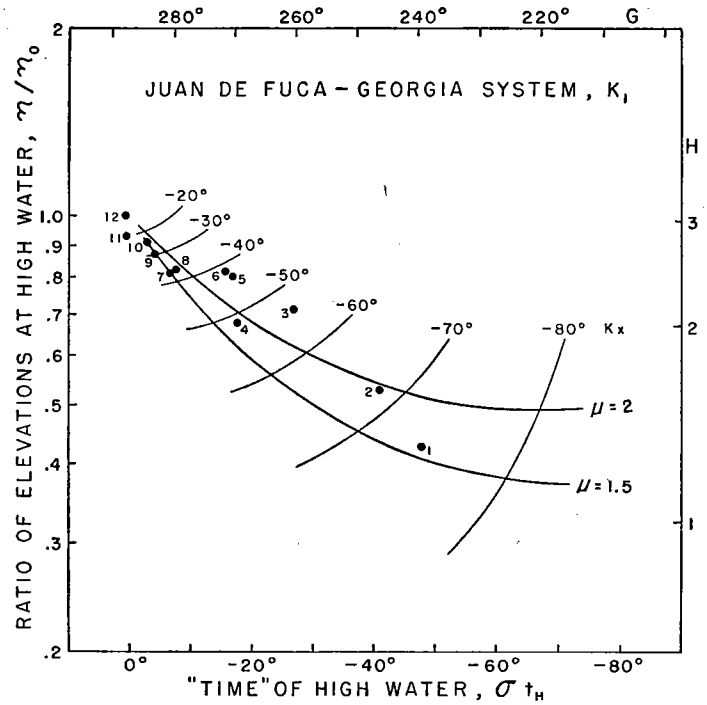

FIG. 12. Analysis of the K_1 component in the Juan de Fuca-Georgia Straits system. To identify the points see Table VI.

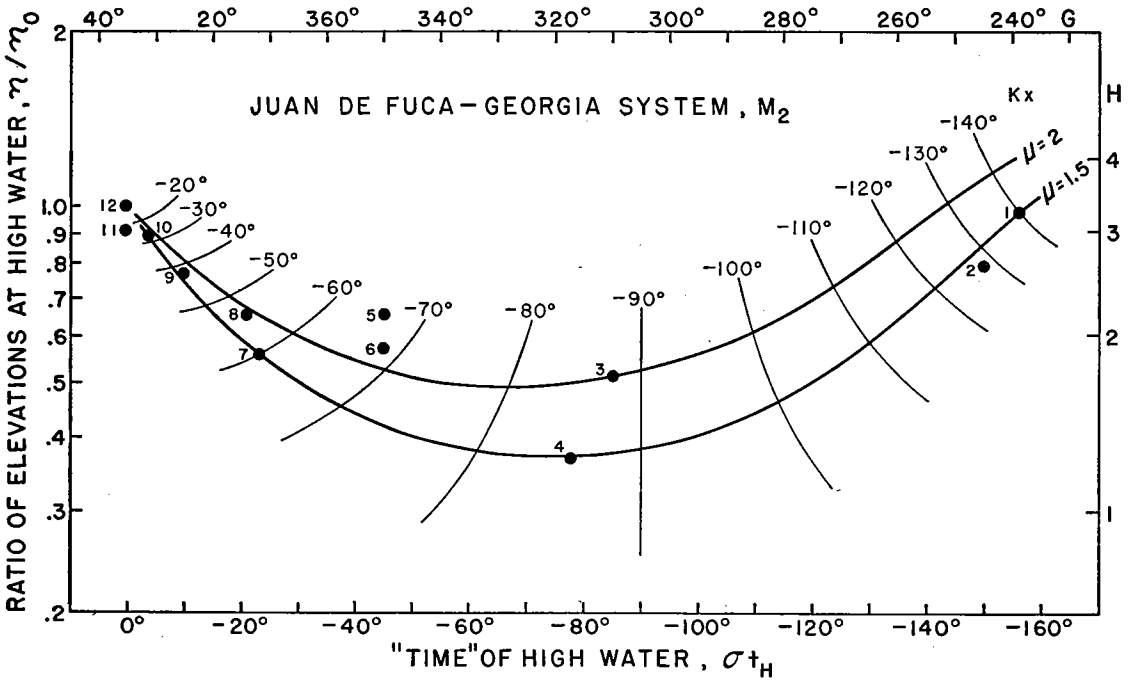

FIG. 13. Analysis of the M_2 component in the Juan de Fuca-Georgia Straits system. To identify the points see Table VI.

The position of the stations is shown in Figure 11 and the analysis of the data for the amplitude of the K_1 and M_2 components and the values of their Greenwich epochs is given in Figures 12 and 13. The reflection point is assumed to be at Whaleton (Station 12), at the head of Georgia Strait. It may be seen that, with the exception of certain anomalous points, to be discussed below, the observed points in the case of both waves fall between coordinates for damping coefficients of 1.5 and 2.0.

TABLE VI

TIDAL DATA FOR JUAN DE FUCA — GEORGIA STRAITS SYSTEM

				K_1			M_2		
				H	*G*	*kx*	*H*	*G*	*kx*
No.	Station	Latitude	Longitude	feet	degrees	degrees	feet	degrees	degrees
1	Claquot	49° 09′	125° 22′	1.29	240	— 74	3.26	239	— 140
2	Neah Bay	48° 22′	124° 37′	1.60	247	— 68	2.67	245	— 128
3	Port Angeles	48° 08′	123° 26′	2.17	261	— 54	1.70	307	— 89
4	Victoria	48° 26′	123° 23′	2.07	270	— 52	1.21	317	— 86
5	Port Townsend	48° 08′	122° 46′	2.46	271	— 43	2.14	350	— 66
6	Reservation Bay	48° 25′	122° 40′	2.51	272	— 42	1.87	350	— 68
7	Friday Harbor	48° 33′	123° 00′	2.49	281	— 38	1.83	12	— 60
8	Bellingham	48° 45′	122° 30′	2.51	280	— 37	2.16	14	— 54
9	Blaine	49° 00′	122° 46′	2.68	284	— 30	2.53	25	— 42
10	Sand Heads	49° 07′	123° 18′	2.79	285	— 24	2.91	31	— 28
11	Point Atkinson	49° 19′	123° 15′	2.83	288	— 20	2.97	35	— 22
12	Whaleton	50° 07′	125° 05′	3.04	288	0	3.31	35	0

From Whaleton the observations extend seaward to Claoquot on the outer coast of Vancouver Island (Station 1) which is taken to represent the wave as it approaches the Strait of Juan de Fuca. The primary wave of the K_1 component undergoes a phase change of 74°, or less than ¼ cycle, within the observed system. In consequence the amplitude of the K_1 component increases continuously as it advances. The primary wave of the M_2 component undergoes a phase change of some 140°, or 4/10 of a cycle, within the channel. Consequently, the amplitude of the M_2 component passes through a minimum near Port Angeles and Victoria where the phase difference from the point of reflection is about 90° or ¼ cycle. At this point the primary and reflected waves of the M_2 component are 180° out of phase and maximal interference occurs.

The position of the cophase lines for the primary wave of the M_2 component is indicated in Figure 11. In the case of the K_1 wave, the distribution would be quite similar, except that the cophase lines would separate phase differences of 5° rather than 10° as drawn for the M_2 wave.

Anomalous observations. The amplitudes of the K_1 and M_2 components at Port Townsend and Reservation Bay (Stations 5 and 6) are greater than the expectation raised for a damping coefficient of 1.5 to 2.0. Since both components are affected alike, this anomalous behavior is to be associated with the geography of the situation. The phenomena may be attributed in part at least to the presence of a Kelvin wave in the Strait of Juan de Fuca. The tide tables show consistently that the mean range of tide is higher along the southern side of the Strait as compared to points on the opposite shore. The effect is most clearly shown by comparing the amplitudes of the K_1 and M_2 components at Port Angeles and Victoria.

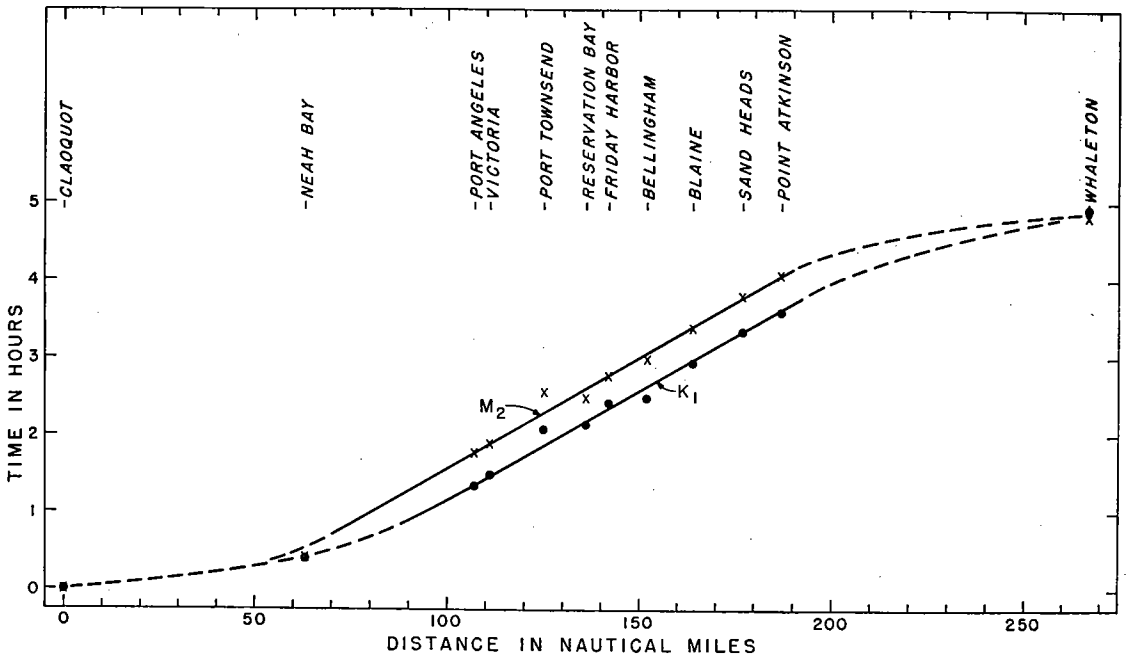

FIG. 14. The times required for the primary waves of the K_1 and M_2 components to traverse the Juan de Fuca-Georgia Straits system.

TABLE VII

INTERVALS BETWEEN HIGH WATER AND SLACK WATER IN JUAN DE FUCA-GEORGIA STRAITS SYSTEM

Current Station	Reference Station for High Water	Phase difference of inflowing wave[1]	Time angle between High Water and Slack Water		Difference
			from theory[2]	from tidal data	
		kx	$\sigma t_H - \sigma t_S$	$G_S - G_H$	
Cape Lazo	Comox	— 8°	14°	— 1°	+ 15°
Bellingham Channel	Eagle Harbor, Cypress Island	— 60°	31°	36°	— 5°
Anacortes, Guemes Channel	Anacortes, Guemes Channel	— 60°	31°	24°	+ 7°
Strawberry Island	Thatcher Pass, Pea Vine Pass	— 60°	31°	42°	— 11°
Pillar Point	Clallam Bay, Crescent Bay	— 110°	122°	121°	+ 1°
Juan de Fuca Strait entrance off Neah Bay	Neah Bay	— 128°	127°	127°	0°

[1] Phase at current station relative to point of reflection.
[2] Estimated assuming $\mu = 1.5$.

The stations where this anomalous behavior occurs are located so as to be influenced by the Puget Sound tidal system which, especially at Port Townsend, may also contribute to the anomalous behavior.

Velocity of the primary wave. From the phase differences of the primary waves of the K_1 and M_2 components at the several stations and the speed number of the waves, the time required for the waves to pass from station to station may be determined. By comparing this information with the distance separating the stations, Figure 14 was prepared, in which the slopes of the curves represent the velocity of the primary waves of the two components along the channel. The time of passage of both waves between Claoquot and Whaleton is almost identical; K_1 requiring 4.92 hours, M_2 requiring 4.83 hours. The velocities of the waves appear to be diminished on entering the Strait of Juan de Fuca and to increase again along the upper part of Georgia Strait[2]. These changes in velocity appear to occur more quickly in the case of the semi-diurnal wave, with the result that this wave is delayed relatively about ½ hour in its passage through the intermediate channels. Within this region, between Port Angeles and Point Atkinson, both waves appear to progress with a velocity which is approximately identical and uniform being about 35 knots.

Time of slack water. Analyzed data do not exist for the determination of the time of slack water of the component waves of the Juan de Fuca-Georgia Straits system. The high water intervals and flood intervals given in the tide and current tables have been employed to determine the interval between high water and slack water for several widely spaced positions along the channel. It is assumed that these intervals apply to a semi-diurnal component with a speed number of 29° per hour. The comparison of the predicted and theoretical phase difference is recorded in Table VII. The agreement is satisfactory when the nature of the basic data is taken into account.

[2] The distance traversed by the primary waves between the time of arrival at Claoquot and at Neah Bay is probably less than that indicated by the geographical distance between these points since the oceanic waves approach the coast at an angle. Consequently, the velocities of passage cannot be estimated reliably until the waves enter the Straits.

Summary. In the Juan de Fuca-Georgia Straits system the general features of both the diurnal and semi-diurnal tidal components are consistently correlated by the theoretical treatment. The primary waves of both components have similar damping coefficients and progress with equal velocities along much of the channel. The channel accommodates 68° of the primary K_1 wave and 128° of the primary M_2 wave between Neah Bay and Whaleton. The changes in the relative values of the diurnal and semi-diurnal components along the channel may be attributed to the differences in the degree of interference between primary and reflected waves of the two species. The primary wave of the semi-diurnal component is maximally suppressed by interference near Victoria and Port Angeles which are about 90° from the head of the system.

The damping coefficient of the diurnal and semi-diurnal components is greater than that found for Long Island Sound and the Bay of Fundy.

DISCUSSION

The method of analysis developed in this paper is based on the dynamical equations for tidal oscillations. Examination of three tidal systems has shown that the principal tidal features may be accounted for satisfactorily by relations deduced from such equations for primary and reflected progressive waves traveling in uniform channels. The failure of irregularities in the form of the channels to distort the relations implies that the primary effect of variations in the cross section of the channel is to alter the rate of the waves' progression. Other effects follow naturally once the effect of velocity on the distribution of phase differences along the channel is taken into account. Thus, in the analysis of the Bay of Fundy system, no explicit consideration has been given to the convergence of the shores and the shoaling of the depths as factors responsible for the increasing range of tide toward the head of the Bay. The analysis reveals directly that the wave moves more slowly as it approaches the head of the Bay and this fact alone is sufficient to account for the distribution of tidal elevations along the channel.

The method of analysis permits estimates to be made of the velocity of the primary and reflected waves. The observation that the primary waves of the diurnal and semi-diurnal components move with the same velocity in the Juan de Fuca-Georgia Straits system is of interest because theoretically the velocity of progressive waves is independent of wave length. However, the relations of velocity to depth are puzzling. In Long Island Sound the primary wave moves at exactly the velocity expected theoretically from the mean depth, as estimated by Marmer (1926). In the Juan de Fuca-Georgia system the velocities are too small, and in the Bay of Fundy too great, relative to the mean depth of the channel. It should be remembered that these estimates refer to the velocities of waves which are mathematical fictions.

The principal anomaly which has appeared in the analyses is that attributed to the rotation of the earth. The method brings out clearly the augmentation of the tidal range along the right side of the advancing wave in practically all systems examined. Theoretically, the slope of the sea surface normal to the direction of the waves advance is proportional to the velocity of the tidal stream. The anomaly should consequently increase with the width of the channel and also with the velocity of the tidal streams at the time when the elevations are measured which is *at high water*. From the relation between high water and of slack water, shown in Figure 5, it is evident that at high water the tidal streams will be greatest at positions where the phase differs by nearly 90° from the point of reflection. Perhaps this is why, in the Long Island Sound system, anomalous effects are observed in Block Island Sound and Fishers Island Sound but not in Long Island Sound proper. In the Strait of Juan de Fuca the greatest contrast in the tidal range on the two sides of the channel is near Victoria and Port Angeles where the phase differs by nearly 90° from the point of reflection.

The successful application of the theory indicates that the basic assumption that the damping of the advancing wave in an irregular channel is directly proportional to the change in phase (and hence inversely proportional to its rate of advance) is essentially correct. It is surprising that a channel as complex, as for example the Juan de Fuca-Georgia Straits, can be treated as though the damping coefficient were constant throughout its length. It is interesting that damping is apparently greater in these Straits than in Long Island Sound and the Bay of Fundy which are shallower. Since the method of analysis supplies a simple means of determining the damping coefficient characteristic

of embayments it opens the way for comparative studies which should reveal the factors on which damping depends.[3]

A preliminary examination of a number of tidal systems other than those treated herein have indicated that in many navigable coastal waters the damping coefficient is of the order of 1.0 to 2.0. In the shallow estuaries which frequently occur at the head of embayments such as the Minas Basin at the head of the Bay of Fundy, and in tidal rivers, the relations of range and time of tide suggest much greater damping if indeed such waters can be properly treated by the theory.

Taylor (1919) has estimated that the tidal wave which enters the Irish Sea loses one-half its amplitude within the cotidal line extending across the channel from Bardsey Island to Arklow Bank. Since this line appears to be about one-quarter wave length from the area of reflection in the North Channel, according to the cotidal chart prepared by Doodson and Corkan (1931), the damping coefficient, μ, for the Irish Sea is approximately 1.4. This value agrees closely with those obtained in the present study.

Damping coefficients of 1.0 and 2.0 imply a reduction in amplitude of the tidal wave of 63 and 86 per cent per cycle, respectively. It is evident that tidal waves suffer very rapid attenuation as has been pointed out by Taylor (1919) and Jeffreys (1923). Consequently, it is not surprising that real tidal systems differ substantially from the idealized frictionless systems commonly used as models in explaining tidal behavior. We will conclude by reviewing the properties of tides in embayments considered as systems undergoing damping of the observed order.

If tides are considered to result from a primary progressive wave, ascending a channel, which is modified by damping and by interference due to reflection, the resulting motion is intermediate in character between that of a progressive and a standing wave.

The tidal behavior depends upon the total change in phase undergone by the primary (and reflected) wave along the length of the channel. As in the case of an ideal standing wave, events change critically at a certain distance from the point of reflection, corresponding to the distance in which the phase change is 90°. If the phase change of the primary wave along the channel is less than 90° the range of tide increases from the entrance to the head of the embayment. If the phase change is greater than 90° the range decreases through a minimum and then increases from this point toward the head of the embayment. The range of tide, however, is not reduced to zero at a nodal line, since this could occur only if interference were complete, a condition which implies the absence of damping. Figure 15 shows the ranges to be expected along channels of different "lengths" assuming a damping coefficient of 1.0. Under these conditions at the position of minimal range the amplitude of the tidal wave is never less than about one-fifth that of the wave at the mouth of the embayment. Only in the absence of damping does the position of minimal range occur where the phase differs by exactly 90° from that at the point of reflection. In real systems it is slightly closer to the point of reflection as may be seen from Figure 2.

[3] The damping of tidal waves is commonly associated with frictional effects due to the roughness of the bottom and with the internal friction of the water itself. In channels it is probable that reflection takes place from the many irregularities of all sizes in the shore line and bottom. Such unsystematic reflection will result in an attenuation of the organized progressive motion of the wave along the channel and will thus contribute to the damping. The damping coefficients deduced in this paper are to be considered in part as the expression of such gross irregularity of the topography as well as the small scale roughness of the bottom. They measure not only the frictional losses but those due to the fact that reflection does not take place from a single barrier; i.e., that the condition of total reflection is not met.

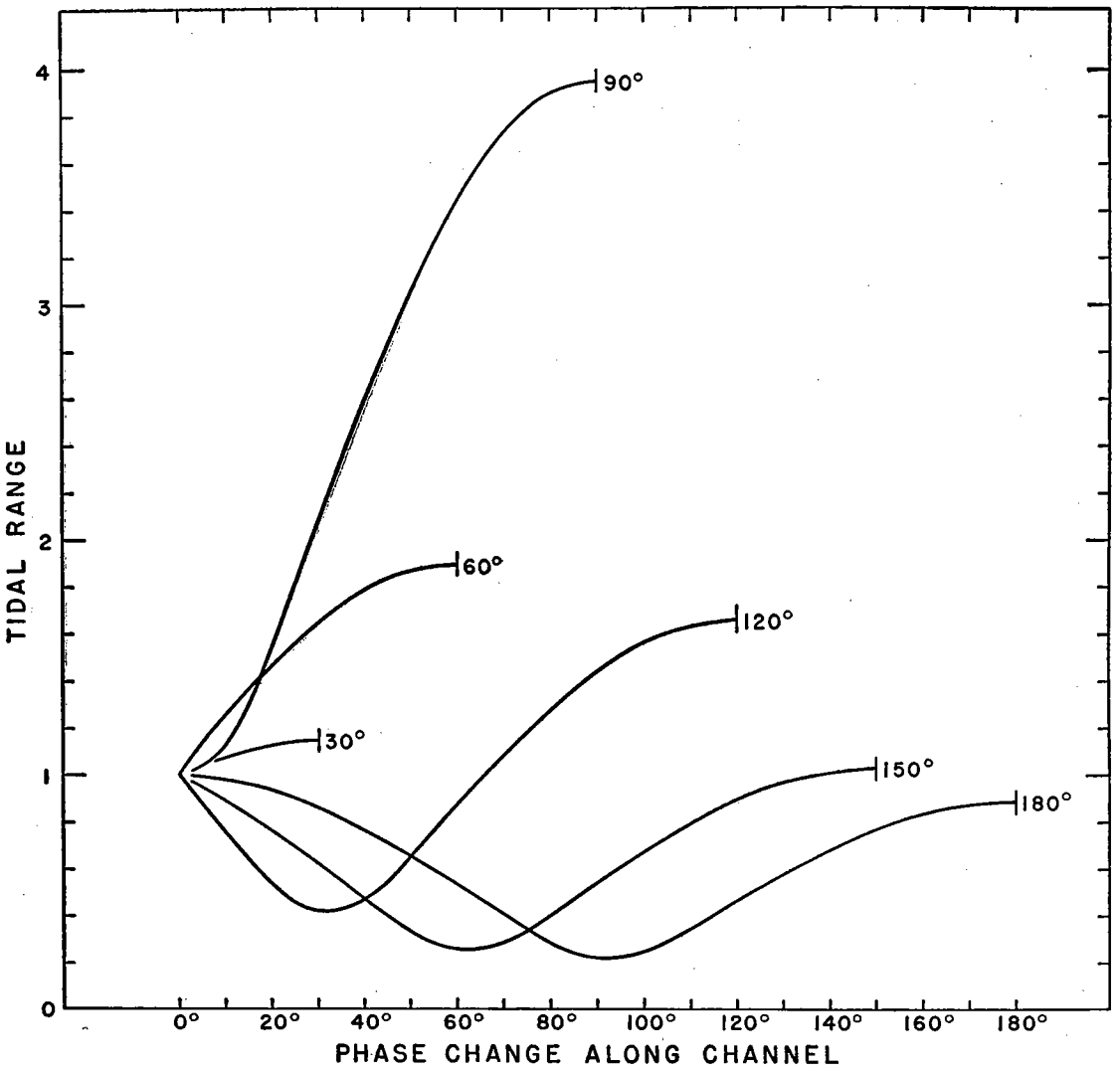

FIG. 15. The amplitude of the tide along a closed channel relative to the amplitude of the tide at the entrance for channels of different length, as measured by the phase change between entrance and barrier. Estimated for a damping coefficient, μ, equal to 1.0.

High water and slack water do not occur at the same time over the entire embayment on either side of the nodal line, as predicted for ideal standing waves. The exact relations are shown in Figures 1 and 5 and are intermediate between those estimated for ideal standing waves ($\mu = 0$) and ideal progressive waves ($\mu = \infty$). At the critical position where the phase difference is 90°, however, the relations are independent of the damping coefficient. High water occurs there one-quarter period earlier than at the head of the embayment, slack water occurs there when it is high water at the head of the embayment.

The augmentation of the tidal range in embayments relative to the range in the outer sea may be attributed to resonance. Doodson and Warburg (1941) have presented a simple qualitative treatment of the tidal elevations in gulfs in which standing waves in

period with the ocean tide occur. They point out that the motions between any sectional plane and the closed end of the channel are indifferent to the circumstances outside this area so long as the proper supplies of energy, kinetic and potential, are forthcoming. It follows from this that an embayment which is shorter than required to permit the development of a complete standing wave having the period of the ocean tide will nevertheless contain a tide having a profile of elevation similar to a portion of the com-

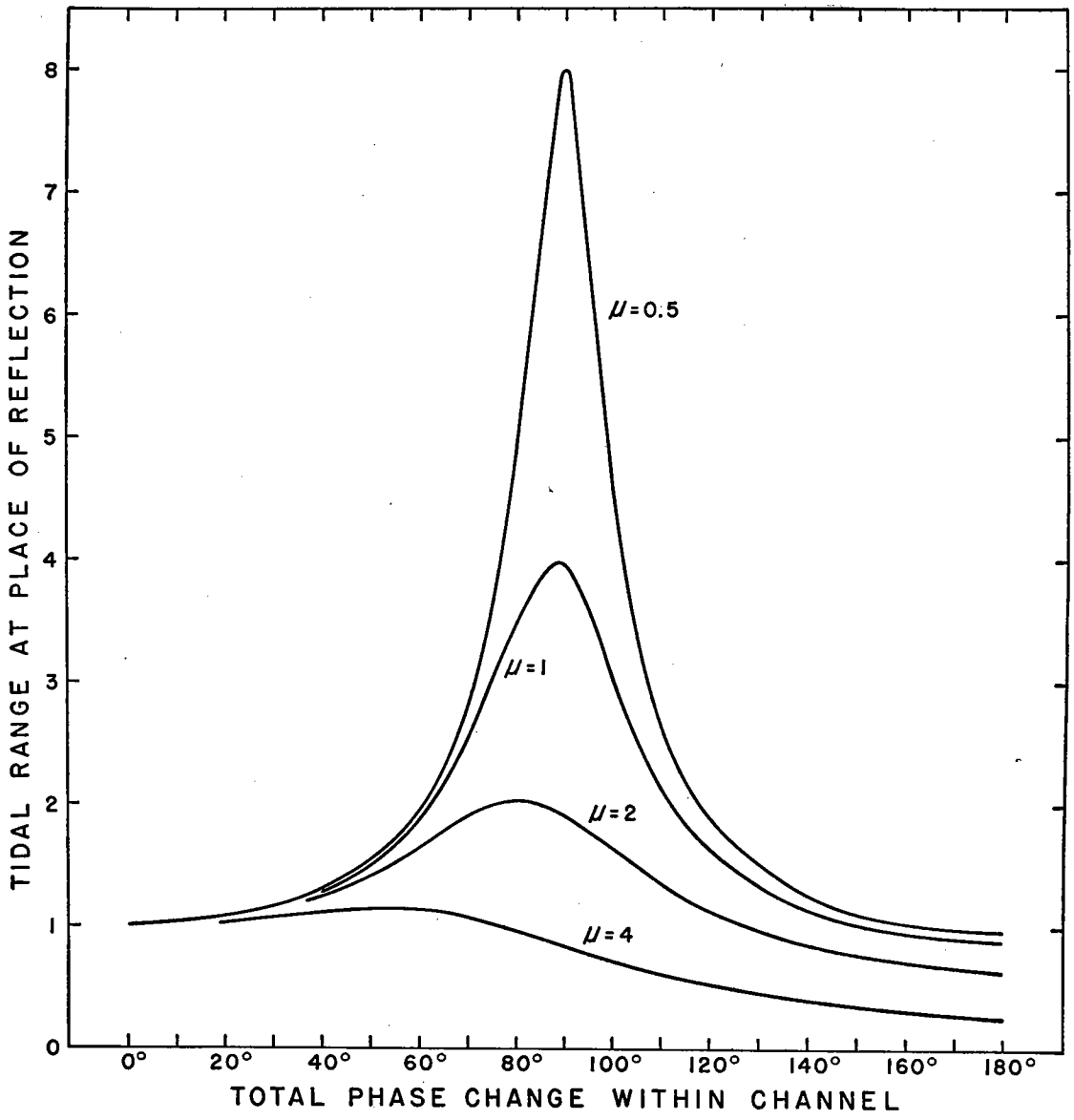

FIG. 16. Amplitude of the tide at the point of reflection relative to the amplitude at the entrance for channels of different length, as measured by the phase change between entrance and barrier, estimated for different values by the damping coefficient, μ.

plete standing wave. The profile is truncated at a sectional plane near the mouth, where the ocean tide provides the proper supplies of energy to maintain the oscillation within the embayment. The ratio of elevations along the gulf are thus fixed by the dimensions of the gulf, their values by the amplitude of the ocean tide.[4]

The treatment developed in the present paper is appropriate to deal with the augmentation of the tide in co-oscillating systems quantitatively and particularly to show the limits placed on resonant amplification by damping such as occurs in natural tidal basins. Equation 5, on which Figures 2 and 4 are based, gives the ratio of the amplitudes of the waves along the channel extending seaward from the point of reflection. What happens along the channel is determined uniquely by what is happening at any point more seaward and on the relations given by the equation. The most seaward point, for purposes of discussion, is at the entrance of the embayment where the ocean wave prevails.

To bring out the relation of the damping coefficient to the augmentation of the range by resonance, the tidal range at the point of reflection, where maximum ranges occur, is shown in Figure 16 for embayments of varied length. The maximum augmentation occurs in embayments in which the phase change between entrance and head is 90° or slightly less. The augmentation is very sensitive to damping and in real embayments where damping coefficients of 1.0 or greater are observed is not more than fourfold. A damping coefficient of 2 does not permit augmentation greater than twofold. Since such increase in amplitude may be due to the conversion of the kinetic energy of the inflowing wave to potential energy at the reflecting barrier, it may be said that resonance is insignificant with damping coefficients of 2 or more.

Finally, it should be pointed out that the relations shown in Figure 16 give the amplitude relative to that of the wave at the entrance to the embayment. There the tidal range may differ widely depending on the situation and will determine in proportion the tidal range within.

It is instructive to compare the range of tide in Long Island Sound and the Bay of Fundy as an illustration of this point. We may consider the Fundy tide to be maintained by the wave observed at Lower East Pubnico and that of the Sound by the wave at Montauk Point. Reflection is assumed to occur at Hopewell Cape and Glen Cove respectively. The phase differences between these points, their ranges and the ratios giving their amplification are given in Table VIII.

It may be seen that the great range of tide observed in the head of the Bay of Fundy is not due to any marked superiority of that bay as a resonating system, since the ratio

TABLE VIII

TIDAL RANGES IN LONG ISLAND SOUND AND BAY OF FUNDY

	kx	Range	Ratio
Long Island Sound			
Glen Cove	0°	7.4 feet	3.7
Montauk Point . . .	— 88°	2.0 "	
Bay of Fundy			
Hopewell Cape . . .	0°	34.3 feet	3.8
Lower East Pubnico . .	— 84°	9.0 "	

[4] "The gulf will affect the tides in the ocean to a certain extent owing to the tidal streams set up across the entrance to the gulf, but the effects will be small if the gulf is small compared to the ocean, and they will be practically localized near the entrance to the gulf. There will be certain adjustments of elevation and stream until the conditions imposed by the gulf are quite satisfied." Doodson and Warburg (1941) p. 165.

of amplfication is essentially the same as in Long Island Sound. The difference is in the range of the tide at the entrance to the embayments. The Long Island Sound system is driven by an oceanic wave, having an amplitude of about three feet along this part of the coast and this wave is reduced somewhat at Montauk Point by interference by reflection from the Sound itself. The Bay of Fundy system, on the other hand, is driven by the tidal system of the Gulf of Maine. Here, the tide is already augmented by those conditions which give the stretch of coast between Nova Scotia and Cape Cod ranges of nine feet or more.

The implication of the foregoing is that where an embayment is tributary to a substantially larger gulf, in which the tidal range is already augmented by the local topography, the tide in the embayment will be further augmented by what may be likened to a two-stage amplification. This may be the explanation of other cases where exceptional tidal ranges occur.

SUMMARY

1. On the assumption that the tides of embayments are the resultant of a primary progressive wave and its reflected counterpart, both undergoing damping, equations are developed relating the tidal range, time of high water, time of slack water, and phase difference of the primary and reflected waves along the channel for given coefficients of damping.

2. These equations may be applied to narrow embayments of simple form in which tidal currents are not rotatory, provided it is further assumed that the effect of irregularities in the cross section of the channel is merely to alter the velocity of propagation of the primary and reflected waves (i.e., to distort the geographical distribution of phase differences), that damping is proportional to the phase change in the primary and reflected waves (rather than to the distance traveled), and that the damping coefficient is constant along the length of the channel.

3. Analysis of the tidal phenomena of Long Island Sound, the Bay of Fundy, and the Juan de Fuca-Georgia Straits system indicate, that the assumptions underlying the equations are sufficiently valid to permit the detailed description of these systems in terms of the distribution of phase differences for the primary and reflected waves along the channel, the velocity of their propagation, and the coefficient of damping.

4. The damping coefficient of navigable embayments is large, representing an attenuation of two-thirds or more per cycle.

5. The departures of tidal behavior in embayments from the behavior of ideal standing waves receive rational and quantitative interpretation.

6. The limits placed by damping on the augmentation of the tidal wave by resonance are quantitatively defined.

7. It is suggested that exceptional tidal ranges observed in such embayments as the Bay of Fundy are due to two or more stages in amplification by the combined effects of reflection and resonance in systems successively tributary to one another and to the ocean.

REFERENCES

AIRY, G. B., 1845: Tides and Waves. Encyclopedia Metropolitana. pp. 241–396. London.

COAST AND GEODETIC SURVEY, U. S. Department of Commerce, 1942: Tidal Harmonic Constants — Pacific and Indian Oceans. Th-2, 134 pp. Washington.

————, 1947: Tide Tables Pacific Ocean and Indian Ocean for the year 1948. Serial No. 697, 405 pp. Washington.

————, 1947: Current Tables Pacific Coast and North America and Philippine Islands for the year 1948. Serial No. 700, 157 pp. Washington.

————, 1948: Tide Tables Atlantic Ocean for the year 1949. Serial No. 706, 325 pp. Washington.

————, 1948: Current Tables Atlantic Coast North America for the year 1949. Serial No. 709, 168 pp. Washington.

DEFANT, A., 1925: Gezeiten probleme des Meeres in Landnähe. Probleme der Kosmischen Physik, VI, pp. 1–80. Hamburg.

DOODSON, A. T. and R. H. CORKAN, 1931: The Principal Constituents of the Tides in the English and Irish Channel. *Phil. Trans. Roy. Soc.* London, A, 231, pp. 29–53.

DOODSON, A. T. and H. D. WARBURG, 1941: Admiralty Manual of Tides. 270 pp. London.

FERREL, W., 1874: Tidal Researches. *U. S. Coast Survey Report*, 1874, Appendix. 268 pp. Washington.

FJELDSTAD, J. E., 1929: Contributions to the Dynamics of Free Progressive Tidal Waves. *Norwegian North Polar Expedition with the* MAUD, 1918–1925, *Scientific Results*, Vol. 4, No. 3, 80 pp.

HARRIS, R. A., 1898: Manual of Tides, Part I. Introduction and Historical Treatment of the Subject. *Report of the Superintendent Coast and Geodetic Survey*, 1897, Appendix No. 8, pp. 319–469. Washington.

————, 1901: Manual of Tides, Part IVA. Outlines of Tidal Theory. *Ibid.*, 1900, Appendix No. 7, pp. 535–700. Washington.

————, 1904: Manual of Tides, Part IVB. Cotidal Lines for the World. *Ibid.*, 1904, Appendix No. 5, pp. 313–400. Washington.

————, 1907: Manual of Tides, Part V. Currents, Shallow Water Tides, Meteorological Tides, and Miscellaneous Matters. *Ibid.*, 1907, Appendix No. 6, pp. 231–545. Washington.

HYDROGRAPHIC AND MAP SERVICE, Department of Mines and Resources, 1940. Tide Tables of the Pacific Coast of Canada. 108 pp. Ottawa.

JEFFREYS, H., 1923: The Tidal Dissipation of Energy. *Nature*, Vol. 112, p. 622.

MARMER, H. A., 1926: The Tide. xi + 282 pp. New York.

PROUDMAN, J. and A. T. DOODSON, 1924: The principal constituent of the tides of the North Sea. *Phil. Trans. Roy. Soc.*, London, A, Vol. 224, pp. 185–219.

TAYLOR, G. L., 1919: Tidal Friction in the Irish Sea. *Phil. Trans. Roy. Soc.*, London, A, Vol. 220, pp. 1–33.

(*Continued from inside front cover*)

Vol. VI,	No. 1.	H. R. Seiwell: Application of the Distribution of Oxygen to the Physical Oceanography of the Caribbean Sea Region, 1938.	0.75†
	No. 2.	R. B. Montgomery: Circulation in Upper Layers of Southern North Atlantic Deduced with Use of Isentropic Analysis, 1938.	0.75†
	No. 3.	H. G. Houghton and W. H. Radford: On the Local Dissipation of Natural Fog, 1938.	1.00*
	No. 4.	H. G. Houghton and W. H. Radford: On the Measurement of Drop Size and Liquid Water Content in Fogs and Clouds, 1938.	0.75*
Vol. VII,	No. 1.	C.-G. Rossby, Jerome Namias, and Ritchie G. Simmers: Fluid Mechanics Applied to the Study of Atmospheric Circulations, Part I. A Study of Flow Patterns with the aid of Isentropic Analysis, 1938.	1.50*
	No. 2.	S. Petterssen and J. M. Austin: Fronts and Frontogenesis in Relation to Vorticity, 1942.	0.75*
	No. 3.	H. R. Seiwell: The Effect of Short Period Variations of Temperature and Salinity on Calculations in Dynamic Oceanography, 1939.	0.75†
	No. 4.	R. B. Montgomery: Observations of Vertical Humidity Distribution above the Ocean Surface and their Relation to Evaporation, 1940.	Out of Print
Vol. VIII,	No. 1.	C. O'D. Iselin: Preliminary Report on Long-Period Variations in the Transport of the Gulf Stream System, 1940.	0.75†
	No. 2.	F. A. Brooks: Observations of Atmospheric Radiation, 1941.	0.50*
	No. 3.	R. A. Allen, R. Fletcher, J. Holmboe, J. Namias and H. C. Willett: Report on an Experiment in Five-Day Weather Forecasting, 1940.	Out of Print
	No. 4.	M. A. Garstens: Some Effects of Shearing Motion on the Propagation of Waves in the Prevailing Westerlies, 1941.	0.75*
Vol. IX,	No. 1.	H. C. Willett: Report of the Five-Day Forecasting Procedure, Verification and Research as Conducted between July, 1940 and August, 1941, 1941.	1.00*
	No. 2.	A. C. Redfield: The Processes Determining the Concentration of Oxygen, Phosphate and other Organic Derivatives within the Depths of the Atlantic Ocean, 1942.	0.50†
	No. 3.	J. M. Austin: Cloudiness and Precipitation in Relation to Frontal Lifting and Horizontal Convergence, 1943.	0.75*
	No. 4.	T. F. Malone: A Study of Interdiurnal Pressure and Temperature Variations in the Free Atmosphere over North America, 1946.	0.75*
Vol. X,	No. 1.	Richard A. Craig: Measurements of Temperature and Humidity in the Lowest 1000 feet of the Atmosphere over Massachusetts Bay, 1946.	0.75†
	No. 2.	Frederick C. Fuglister: Average Monthly Sea Surface Temperatures of the Western North Atlantic Ocean, 1947.	0.50†
	No. 3.	Gardner Emmons: Vertical Distributions of Temperature and Humidity over the Ocean between Nantucket and New Jersey, 1947.	1.00†
	No. 4.	H. R. Seiwell: Results of Research on Surface Waves of the Western North Atlantic, 1948.	1.00†
Vol. XI,	No. 1.	A. F. Bunker, B. Haurwitz, J. S. Malkus, and H. Stommel: Vertical Distribution of Temperature and Humidity over the Caribbean Sea, 1949.	1.00†
	No. 2.	Henry C. Stetson: The Sediments and Stratigraphy of the East Coast Continental Margin; Georges Bank to Norfolk Canyon, 1949.	1.00†
	No. 3.	William S. von Arx: An Electromagnetic Method for Measuring the Velocities of Ocean Currents from a Ship Under Way, 1950.	1.00†
	No. 4.	Alfred C. Redfield: An Analysis of Tidal Phenomena in Narrow Embayments, 1950.	1.00†

* Requests for this number should be addressed to Meteorological Department, Massachusetts Institute of Technology, Cambridge, Massachusetts.

† Requests for this number should be addressed to Woods Hole Oceanographic Institution, Woods Hole, Massachusetts.